Research Report

CfrA, a Novel Carbon Flow Regulator, Adapts Carbon Metabolism to Nitrogen Deficiency in Cyanobacteria[1[OPEN]]

M. Isabel Muro-Pastor,[2,3] Áureo Cutillas-Farray,[4] Laura Pérez-Rodríguez,[4] Julia Pérez-Saavedra,[4,5] Ana Vega-de Armas,[6] Ana Paredes,[7] Rocío Robles-Rengel, and Francisco J. Florencio[2]

Instituto de Bioquímica Vegetal y Fotosíntesis, Consejo Superior de Investigaciones Científicas–Universidad de Sevilla, 41092 Sevilla, Spain

ORCID IDs: 0000-0001-7366-7904 (M.I.M.-P.); 0000-0002-7585-695X (A.C.-F.); 0000-0003-1987-6195 (L.P.-R.); 0000-0003-0829-6056 (J.P.-S.); 0000-0001-9725-2818 (A.V.-d.A.); 0000-0003-3119-8788 (A.P.); 0000-0002-5738-4880 (R.R.-R.); 0000-0002-2068-7861 (F.J.F.).

Cyanobacteria unable to fix atmospheric nitrogen have evolved sophisticated adaptations to survive to long periods of nitrogen starvation. These genetic programs are still largely unknown—as evidenced by the many proteins whose expression is regulated in response to nitrogen availability, but which belong to unknown or hypothetical categories. In *Synechocystis* sp. PCC 6803, the global nitrogen regulator NtcA activates the expression of the *sll0944* gene upon nitrogen deprivation. This gene encodes a protein that is highly conserved in cyanobacteria, but of unknown function. Based on the results described herein, we named the product of *sll0944* carbon flow regulator A (CfrA). We analyzed the phenotypes of strains containing different levels of CfrA, including a knock-out strain (ΔcfrA), and two strains overexpressing CfrA from either the constitutive P_{trc} promoter (Ptrc-cfrA) or the arsenite-inducible promoter P_{arsB} (Pars-cfrA). Our results show that the amount of CfrA determines the accumulation of glycogen, and affects the synthesis of protein and photosynthetic pigments as well as amino acid pools. Strains with high levels of CfrA present high levels of glycogen and a decrease in photosynthetic pigments and protein content when nitrogen is available. Possible interactions between CfrA and the pyruvate dehydrogenase complex or PII protein have been revealed. The phenotype associated with CfrA overexpression is also observed in PII-deficient strains; however, it is lethal in this genetic background. Taken together, our results indicate a role for CfrA in the adaptation of carbon flux during acclimation to nitrogen deficiency.

Cyanobacteria have recently gained interest for their ability to sequester and transform CO_2 to high-value products using solar energy, offering a renewable resource to produce green chemicals and biofuel (Oliver et al., 2016). As they exhibit great metabolic plasticity, strategies aimed at engineering their metabolism have emerged to overcome the current environmental crisis. (Angermayr et al., 2009; Qian et al., 2018). The non-diazotrophic unicellular cyanobacterium *Synechocystis* sp. PCC 6803 (hereafter: *Synechocystis*) is one of the most extensively studied model cyanobacteria. A large quantity of genomic, biochemical, and metabolic data are available for this organism (Knoop et al., 2010; Kopf et al., 2014), which has become a perfect chassis for synthetic biology (Berla et al., 2013).

In *Synechocystis*, different nitrogen compounds are converted to ammonium before their incorporation into 2-oxoglutarate (hereafter: 2-OG) through the glutamine synthetase-glutamate synthase (GS-GOGAT) cycle. Two enzymes with glutamine synthetase activity are present in *Synechocystis*, the housekeeping enzyme Gln synthetase I (GSI; *glnA*) and GSIII (*glnN*) expressed mainly in nitrogen deficiency (Muro-Pastor et al., 2005; Esteves-Ferreira et al., 2018). Both Gln and Glu are the major donors of amino groups for the synthesis of additional amino acids and many other nitrogen-containing compounds. Additionally, because the carbon skeleton for ammonium assimilation, 2-OG, is a tricarboxylic acid cycle intermediate, it constitutes the central crossroad for nitrogen and carbon (C/N) metabolism (Zhang et al., 2018) and is the status reporter of the C/N balance in cyanobacteria (Muro-Pastor et al., 2001).

Regarding central carbon metabolism, cyanobacteria have very complex metabolic circuits that are both robust (allowing a stable distribution of the flux) and flexible (able to adapt to changing environmental conditions; Xiong et al., 2017). One of the strategies used for this purpose is the synthesis of carbon storage compounds such as glycogen. This mechanism allows survival under different stress conditions such as nutrient starvation and makes it possible for *Synechocystis* to grow in diurnal light–dark cycles (Luan et al., 2019).

One of the key elements in the control of C/N homeostasis in cyanobacteria is NtcA, a global transcriptional regulator that can act as activator or repressor (Herrero et al., 2001). In *Synechocystis*, NtcA regulates both the GS-GOGAT cycle (*glnA* and *glnN*) and the carbon skeleton supply. GSI expression and activity are tightly regulated (Bolay et al., 2018), its expression is induced under nitrogen limitation and its activity is controlled by direct interaction with two inactivating factors (IF7 and IF17 encoded by *gif* genes; García-Domínguez et al., 1999).

The 2-OG plays a central role in a complex regulatory network as the effector of different regulators, including NtcA or the widely distributed PII signal transduction protein. 2-OG directly binds NtcA linking its function with nitrogen status but maximal activation of NtcA also requires the binding of the coactivator PII interacting protein (PipX), which mutually exclusively binds to either NtcA or PII (Forchhammer and Selim, 2020).

In the absence of combined nitrogen, the GS-GOGATI cycle is not able to cope with the supply of 2-OG, which results in increased levels of this metabolite (Muro-Pastor et al., 2001). This increase reports an imbalance in the nitrogen state that activates NtcA, which triggers the metabolic adaptation to nitrogen starvation known as "chlorotic response" or "bleaching" (Giner-Lamia et al., 2017). This process includes a rapid degradation of phycobilisomes (cyanobacterial light-harvesting complexes), which releases amino acids required for the synthesis of stress acclimation proteins (Forchhammer and Schwarz, 2019). Another immediate response to nitrogen starvation is the accumulation of glycogen, which serves as carbon sink for the fixed CO_2 (Gründel et al., 2012). When nitrogen starvation persists, cells gradually enter a quiescent state with minimum photosynthetic activity and arrested cell growth, which allows them to survive long periods of time in these conditions (Spät et al., 2018). This process is reversible, and chlorotic cells can efficiently return to vegetative growth upon nitrogen availability (Klotz et al., 2016).

Many high-throughput studies have addressed the process of adaptation to nitrogen deficiency in different cyanobacteria, and many genes and proteins of unknown function have been identified as possibly involved in this sophisticated adaptation strategy (Krasikov et al., 2012; Hasunuma et al., 2013; Osanai et al., 2014a; Spät et al., 2015, 2018; Choi et al., 2016; Carrieri et al., 2017; Giner-Lamia et al., 2017). A global study of the NtcA regulon of *Synechocystis* provided an overview of the genes whose expression depends on this regulator (Giner-Lamia et al., 2017), although many of them belong to hypothetical categories. One of these genes is *sll0944*, whose expression is positively regulated by NtcA and significantly induced during the first stages of acclimation to nitrogen starvation (Osanai et al., 2006, 2014a; Giner-Lamia et al., 2017). Recently it has also been linked to the C/N regulatory protein PII (Watzer et al., 2019). This gene currently lacks annotation and belongs to the group of conserved hypothetical genes with a wide phyletic distribution.

In this work we have carried out a characterization of the protein encoded by *sll0944*, which, based on our results, we have named "carbon flow regulator A" (CfrA). A physiological and metabolic study of *Synechocystis* strains with different levels of CfrA has allowed us to conclude that it is involved in the modulation of carbon flow that takes place during adaptation to nitrogen starvation.

RESULTS

CfrA Is a Highly Conserved Protein Exclusive of Cyanobacteria

A search of CfrA homologs revealed that this protein is widely distributed among cyanobacteria and seems exclusive to this phylum. Figure 1A shows an alignment of CfrA homologous sequences from some cyanobacteria. This alignment shows a highly conserved region that constitutes the unknown function domain DUF1830 followed by a variable region. In the case of *Synechocystis* CfrA, the DUF1830 domain extends between Cys-18 and Ile-83. This analysis, together with the previous one of the promoter region of *sll0944* (Giner-Lamia et al., 2017), reveals a misannotation of the CfrA protein in the Uniprot database (https://www.uniprot.org/uniprot/P77971). The protein has a molecular mass of 12 kD and a theoretical pI of 4.2. A representation of the identity of the residues for each of the positions of the DUF1830 domain in all the available sequences using WebLogo (Crooks et al., 2004) is shown in Figure 1B, and a compilation of these sequences is provided (Supplemental Dataset S1). We have also carried out ab-initio models of CfrA structure using the prediction tool ROSETTA (Song et al., 2013). All the generated models were quite consistent in the

[1]This work was supported by Ministerio de Economía y Competitividad (grant no. BFU2013–41712), Agencia Estatal de Investigación (grant no. BIO2016–75634–P), the Junta de Andalucía (grant no. BIO–0284), the FFondo Europeo de Desarrollo Regional, the Consejo Superior de Investigaciones Científicas (Junta para Ampliación de Estudios e Investigaciones Científicas-Intro fellowship no. JAEINT–18 –01250 to A.C.-F.), the University of Sevilla (contract no. USE–15794 –Q to J.P.-S.), the Ministerio de Educación, Cultura y Deporte (Collaboration Scholarship to A.P.), and the Ministerio de Economía y Competitividad (Ayudas para la Formación de Pofesorado Universitario fellowship no. AP2010–0366 to R.R.-R.).

[2]Senior authors.

[3]Author for contact: imuro@ibvf.csic.es.

[4]These authors contributed equally to this article.

[5]Present address: Institut de Recerca Biomèdica, Carrer de Baldiri Reixac 10, 08028 Barcelona, Spain.

[6]Present address: Madrid Institutes for Advanced Studies Energía, Avenida Ramón de la Sagra, 3, 28935 Móstoles, Madrid, Spain.

[7]Present address: Centro Nacional de Investigaciones Cardiovasculares, Calle Melchor Fernández Almagro 3, 28029 Madrid, Spain.

The author responsible for distribution of materials integral to the findings presented in this article in accordance with the policy described in the Instructions for Authors (www.plantphysiol.org) is: M. Isabel Muro-Pastor (imuro@ibvf.csic.es).

M.I.M-P. performed the experiments and analyzed the data together with A.C.-F., L.P.-R., J.P.-S., A.V.-d.A., and A.P. (undergraduate or master students); M.I.M.-P. and F.J.F. conceived and designed the experiments, supervised the work, and analyzed the data; R.R.-R. constructed the ΔglnB strain; M.I.M.-P. wrote the article with contributions of all the authors; M.I.M.-P. agrees to serve as the author responsible for contact and ensures communication.

[OPEN]Articles can be viewed without a subscription.

www.plantphysiol.org/cgi/doi/10.1104/pp.20.00802

region corresponding to the DUF1830 domain. Images of tertiary structure and surface hydrophobicity of CfrA, obtained using the program UCSF Chimera (Pettersen et al., 2004), are shown in Figure 1, C and D, respectively.

CfrA Is Expressed during Early Acclimation to Nitrogen Starvation

sll0944, encoding CfrA, was identified as a member of the NtcA regulon whose transcription is upregulated after nitrogen depletion (Giner-Lamia et al., 2017). This expression pattern has been observed for CfrA homologs in other cyanobacteria (Mitschke et al., 2011; Choi et al., 2016). To monitor the cellular level of CfrA, we produced specific antibodies against this protein (Supplemental Methods S1). Cells of the *Synechocystis* wild-type strain were grown under standard conditions until exponential growth phase, and then incubated in nitrogen-free medium. As shown in Figure 2A, CfrA was undetectable in nitrate-growing cells and accumulated early after nitrogen removal. This accumulation reached its maximum in the first 24 h of nitrogen deficiency and decreased after 48 h in these conditions, with minimum levels at the end of the analyzed period (144 h). Then, sodium nitrate was added at the standard concentration in BG11C. CfrA accumulated again during the first 24 h in these conditions, and then it progressively decreased to the undetectable level characteristic of nitrate growth.

To investigate the effect of CfrA accumulation under nitrogen sufficiency, in which it is not naturally expressed, we generated a construct where the *cfrA* open reading frame (ORF) was placed under the control of P_{trc} promoter, a nitrogen-independent constitutive promoter in *Synechocystis* (Guerrero et al., 2012; Table 1; Supplemental Fig. S1). The Ptrc-cfrA strain was analyzed in the same conditions described above for the wild type. As expected, the Ptrc-cfrA strain accumulated high levels of CfrA in the presence of nitrate (Fig. 2B), and this accumulation was maintained during the first 48 h of nitrogen deficiency although it subsequently decreased to minimum levels in chlorotic cells (120 to 144 h of nitrogen deficiency). When nitrate was re-added to chlorotic cells, CfrA protein accumulated again at high levels that were maintained throughout the analyzed period. The accumulation of the housekeeping protein GSI used as control did not experience substantial changes throughout the chlorosis process and its reversion. However, its accumulation appears to be slightly less in the CfrA-overexpressed strain.

CfrA Expression Levels Influence the Rate of Chlorosis Reversion

Because CfrA expression is induced during adaptation to nitrogen deficiency (Fig. 2A), we analyzed in more detail the process of chlorosis and its reversion in strains with different levels of CfrA. Wild-type, ΔcfrA, and Ptrc-cfrA strains were compared. As shown in Figure 3A, after 13 d of nitrogen starvation, absorption spectra of the three strains were almost identical and showed the characteristic degradation of the photosynthetic pigments of the chlorotic cells, demonstrating that the CfrA protein is not required for the bleaching process. However, when nitrate was added, a clear difference was observed in the awakening of the three strains, indicating that CfrA expression levels affect resuscitation after chlorosis. In fact, the *cfrA* knock-out strain (ΔcfrA) regreened faster than the wild-type, whereas the overexpressing strain (Ptrc-cfrA) did it more slowly (Fig. 3, B–D). The maximum difference in pigmentation was observed 48 h after the addition of nitrate to the chlorotic cells (Fig. 3, C and D). Additionally, it was observed that the time required for greening was shorter in all the strains when the chlorosis period decreased (Supplemental Fig. S2).

Glycogen Concentration Is Dependent on CfrA Levels in *Synechocystis*

Because in *Synechocystis* glycogen begins to accumulate almost immediately upon nitrogen depletion (Luan et al., 2019), we wanted to assess whether CfrA expression levels affected the accumulation of this polymer. We placed the *cfrA* gene under the nitrogen-independent, arsenite-inducible promoter of the *arsBHC* operon of *Synechocystis*, which shows high ON/OFF ratio (López-Maury et al., 2003) and constructed the Pars-cfrA strain (Table 1; Supplemental Fig. S1). To analyze this strain, it was first propagated without arsenite in BG11C medium and then flasks were inoculated at 0.3 OD_{750} in the presence of increasing arsenite concentrations (1, 5, 10, 20, 50, 200, and 500 μM). A control culture without arsenite was also included. After 24 h in the presence of arsenite, samples were collected and the accumulation of CfrA and glycogen was analyzed. As shown in Figure 4A, an arsenite-dependent CfrA accumulation was observed in this strain. While *cfrA* overexpression in these conditions did not affect cell growth (Fig. 4B), the glycogen concentration increased proportionally to the amount of CfrA (Fig. 4C). We quantified up to a 12-fold increase of glycogen content in the presence of 500 μM of arsenite compared to the control sample. As an indication of the C/N balance and of carbon flux toward the tricarboxylic acid cycle, we also measured glutamine synthetase (GS) activity, which slightly decreased with increasing arsenite concentrations (Fig. 4D). To ensure maximum induction of CfrA in the experiments that follow, 1 mM of arsenite was used.

The Level of CfrA Affects Glycogen Content without Altering the Accumulation of the Glycogen Synthesis Enzymes GlgC and GlgA1

Once it was determined that the amount of CfrA affects the accumulation of glycogen, we compared the wild-type, ΔcfrA, and Pars-cfrA strains to test whether

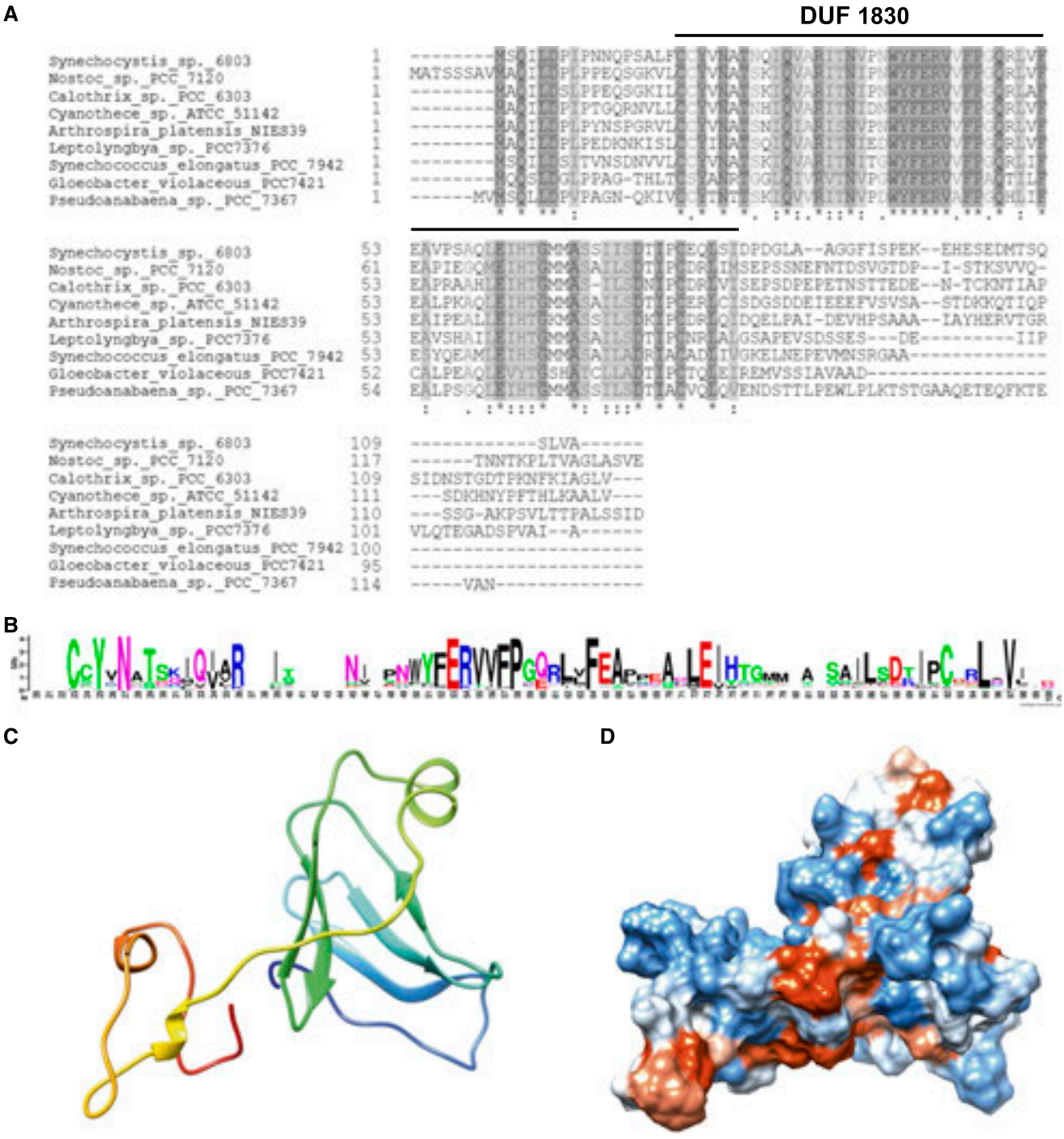

Figure 1. Sequence and structural analysis of CfrA. A, Sequence alignment of several CfrA homologous proteins from representative cyanobacteria. The asterisks denote identical residues in all aligned sequences, shaded in dark gray; the colons denote residues with a strong conservation, shaded in medium gray; and the periods denote weakly conserved residues, shaded in light gray. B, WebLogo representing the identity of amino acid residues for each of the positions of the DUF1830 domain in all the sequences available in the databases. C and D, Ab initio structural model of CfrA generated by the program ROSETTA (Song et al., 2013). Images of CfrA structure, using the program UCSF Chimera (Pettersen et al., 2004), are represented as both tertiary structure ribbon representation, colored from blue (N terminus) to red (C terminus; C), and surface hydrophobicity map from blue for the most hydrophilic, to white, to orange-red for the most hydrophobic (D).

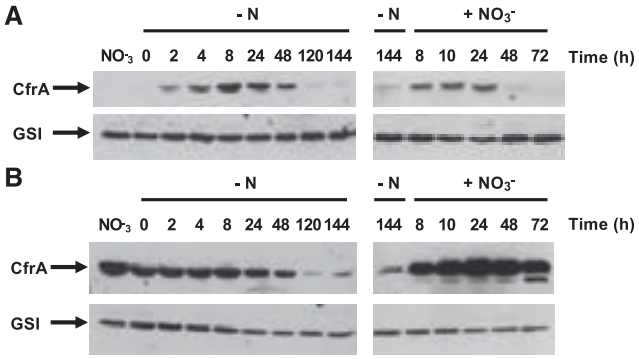

Figure 2. Accumulation of CfrA in different *Synechocystis* strains through the chlorosis process and its reversion. Samples from the wild-type (A) or the Ptrc-cfrA (B) strains were taken from cells growing with nitrate as nitrogen source (NO_3^-), after the elimination of the nitrogen source (−N) and after readdition of this source ($+NO_3^-$) at the indicated times. Total protein crude extracts were obtained from cells corresponding to 2 OD_{750} in every case. Equal volumes of each extract were loaded, resolved on SDS-PAGE, blotted, and incubated with anti-CfrA antibodies. The samples from 144 h of nitrogen starvation (−N) were loaded in both gels as a control. Membranes were incubated also with anti-GSI antibodies as control of a housekeeping protein.

the observed phenotype for the overexpressing strain (Fig. 4) was maintained or enhanced in the presence of additional carbon supply. The strains were first propagated in flasks and then 150-mL cultures were inoculated under standard conditions in BG11C at 0.3 OD_{750} and supplemented with 1% (v/v) CO_2. When these cultures reached ~1 OD_{750}, 1 mM of arsenite was added to all three strains, to discard arsenite-dependent phenotypic effects, and samples were collected for the analysis of cell growth, GS activity, and glycogen content (Fig. 5).

We could detect an early overexpression of CfrA in Pars-cfrA strain, reaching its maximum already 6 h after arsenite addition while CfrA was not detected in the wild-type strain (Fig. 5A). A decrease in total protein content was also observed in crude extracts from Pars-cfrA cells with time (Fig. 5, A, D, and F). Growth rates did not differ significantly in the tested strains when compared to wild type, although for Pars-cfrA there was a slight increment in OD_{750} when compared to the other two strains (Fig. 5B). As it is shown in Figure 5C, 24 and 72 h after CfrA overexpression, GS activity significantly decreased for Pars-cfrA in comparison to the wild type, while no significant effect was observed for the knock-out mutant ΔcfrA. Western-blot analysis of GSI, GSIII, and NtcA proteins showed a decrease in all these proteins associated with CfrA overexpression. In fact, GSIII protein was almost undetectable in the Pars-cfrA strain after arsenite addition (Fig. 5D).

Regarding glycogen, Pars-cfrA accumulated more than 16-fold at 24 h and more than 8-fold at 72 h in comparison to the wild type, while *cfrA* deletion caused a small decrease in glycogen concentration when compared to wild-type levels (Fig. 5E). To test whether glycogen accumulation was related to an increase in the expression of enzymes involved in glycogen synthesis, we analyzed ADP-Glc pyrophosphorylase (GlgC) and glycogen synthase I (GlgA1) expression in the three strains. No significant differences in the accumulation of these enzymes were observed. Only a small decrease in the amount could be observed in the Pars-cfrA strain after 48 h of arsenite addition, coincident with a general decrease in the protein content observed by Coomassie blue staining (Sigma-Aldrich) of the cell extracts (Fig. 5F).

Table 1. Synechocystis *strains used in this work*

Name	Description
Wild type	*Synechocystis* sp. PCC 6803 wild type
ΔcfrA	Δ*cfrA*::*aadA*$^+$, Sm/Sp^r
Ptrc-cfrA	Δ*cfrA*::*aadA*$^+$, *nrsD*::P_{trc}-*cfrA*:*npt*, Sm/Sp^r, Km^r
Pars-cfrA	Δ*cfrA*::*aadA*$^+$, *nrsD*::P_{arsB}-*cfrA*:*npt*, Sm/Sp^r, Km^r
ΔglnB	Δ*glnB*::*cm*, Cm^r
ΔglnB/Pars-cfrA	Δ*glnB*::*cm*, *nrsD*::P_{arsB}-*cfrA*:*npt*, Cm^r, Km^r

Photosynthetic Pigment Concentrations Are Also Affected by CfrA Accumulation

A clear change in the color of the Pars-cfrA strain was noted after arsenite addition. These cultures appeared less blue-green than the wild-type or the ΔcfrA cultures. We analyzed and compared the absorption spectra of the three strains before and after 24 or 72 h of arsenite addition. We could observe a notable decrease in absorbance at 678 and 625 nm in the case of the overexpressing strain (Fig. 6A). Quantification of the differences in absorbance of the 678-, 625-, and 485-nm peaks, which are indicative of chlorophyll, phycobilin, and carotenoid contents, respectively, is shown in Figure 6, B to D. A significant decrease in chlorophyll content was observed in the case of Pars-cfrA strain, while a very subtle increase was observed for the knock-out strain (Fig. 6B). As shown in Figure 6C, there was a significant decrease of phycobilins with CfrA overexpression, while the deletion of *cfrA* caused a small increase in the content of this pigment (Fig. 6C). With respect to carotenoids, there was a first decay 24 h after CfrA induction in Pars-cfrA, but carotenoid content returned to wild-type levels after 72 h. However, no significant changes were observed for ΔcfrA (Fig. 6D).

Using confocal laser microscopy, a notable decrease of auto-fluorescence (shown in red) was noticed in the Pars-cfrA strain respect to the others. Interestingly, we could also observe that cells of this strain were slightly larger than those of the other two strains, although due to the small size of *Synechocystis* cells (~2 μm), a more detailed study would be required to confirm whether these differences are significant (Fig. 6E).

CfrA Accumulation Affects Amino Acid Content

To analyze the set of amino acids in the Pars-cfrA strain, we proceeded as in previous experiments

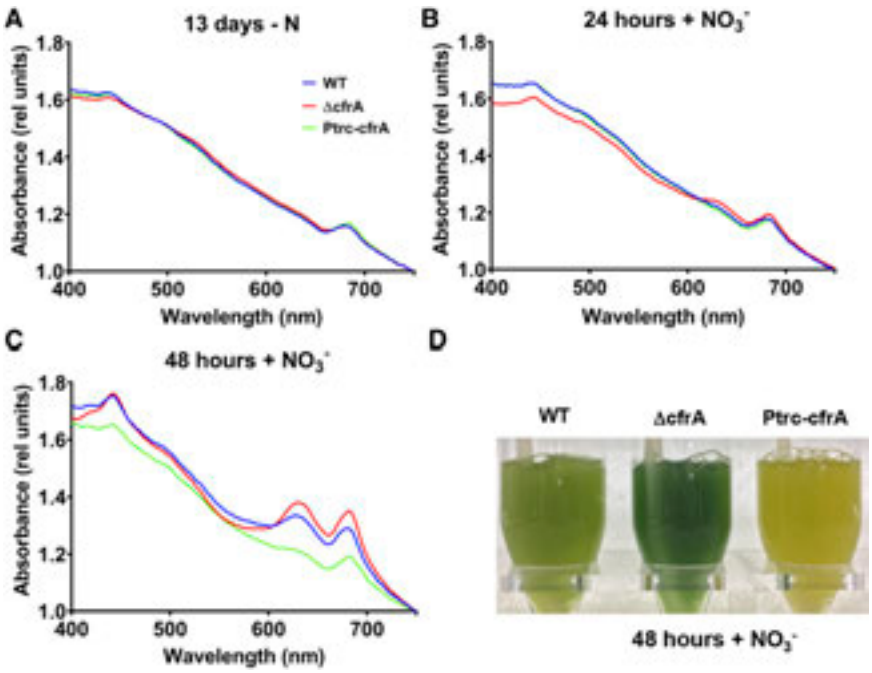

Figure 3. Evolution of pigmentation during resuscitation of chlorotic cells. A to C, Absorption spectra (400 to 750 nm) of *Synechocystis* cultures from wild-type, ΔcfrA, and Ptrc-cfrA strains during resuscitation. After 13 d of nitrogen starvation (−N), sodium nitrate (17.6 mM) was added to cultures and spectra were performed at the indicated times ($+NO_3^-$). Spectra were normalized to the same optical density at 750 nm of 1. D, Image of wild-type (WT), ΔcfrA, and Ptrc-cfrA *Synechocystis* strains after 48 h of sodium nitrate addition. A representative experiment of several independent replicates is shown.

(Fig. 5), but by comparing cultures of Pars-cfrA strain in the absence (−) or presence (+) of 1 mM of arsenite. We quantified the 20 amino acids in both cultures and compared their levels at different times after arsenite addition. A control of the already described phenotype of Pars-cfrA in this experiment is shown in Supplemental Figure S3.

As shown in Figure 7, we observed a significant increase in the Ala and Ser pools 24 h after the induction of CfrA. However, after 48 h the content of these amino acids started to decline. Arg and Trp contents in Pars-cfrA (+) experienced a reduction of 73% and 70%, respectively, when compared to Pars-cfrA (−). CfrA overexpression also reduced the levels of Thr, Lys, and Glu ~50%. There was a small reduction of Cys, His, Phe, Gln, Asp, and Asn pools, while the contents of the remaining amino acids were not significantly different in both cultures.

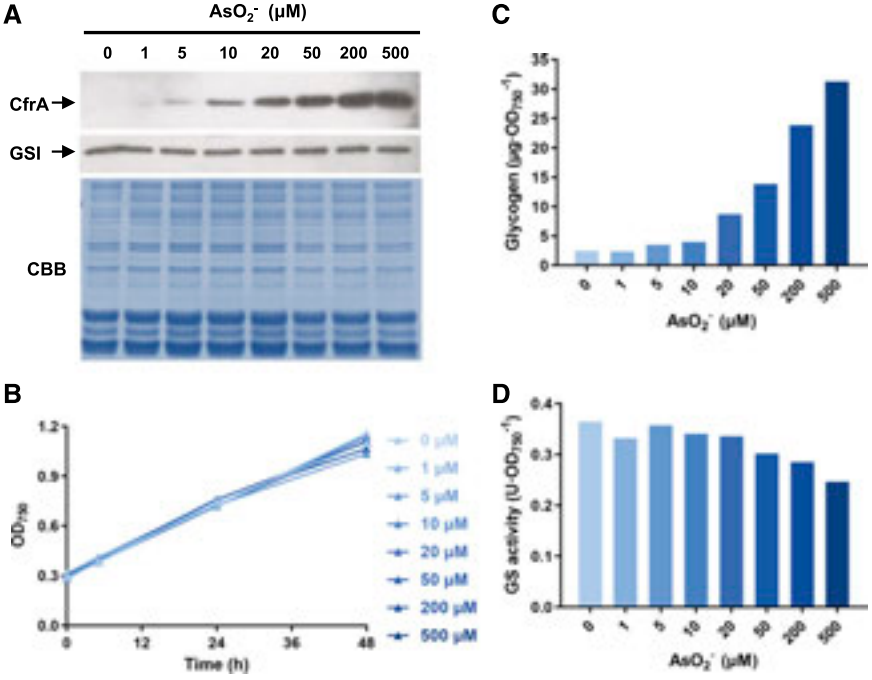

Figure 4. Analysis of Pars-cfrA strain with increasing arsenite concentrations. A, Western-blot analysis of CfrA and GSI in Pars-cfrA after 24-h growth with increasing arsenite (AsO_2^-) concentrations (0, 1, 5, 10, 20, 50, 200, and 500 μM). Total protein crude extracts were obtained from cells corresponding to 2 OD_{750} in every case. Equal volumes of each extract were loaded. Coomassie Brilliant Blue (CBB) staining is shown as a protein loading control. B, Growth analysis of Pars-cfrA cultures grown with increasing arsenite concentrations. C and D, Glycogen content (C) and GS activity (D) of Pars-cfrA cultures after 24-h growth with increasing arsenite concentrations. A representative experiment of several independent replicates is shown.

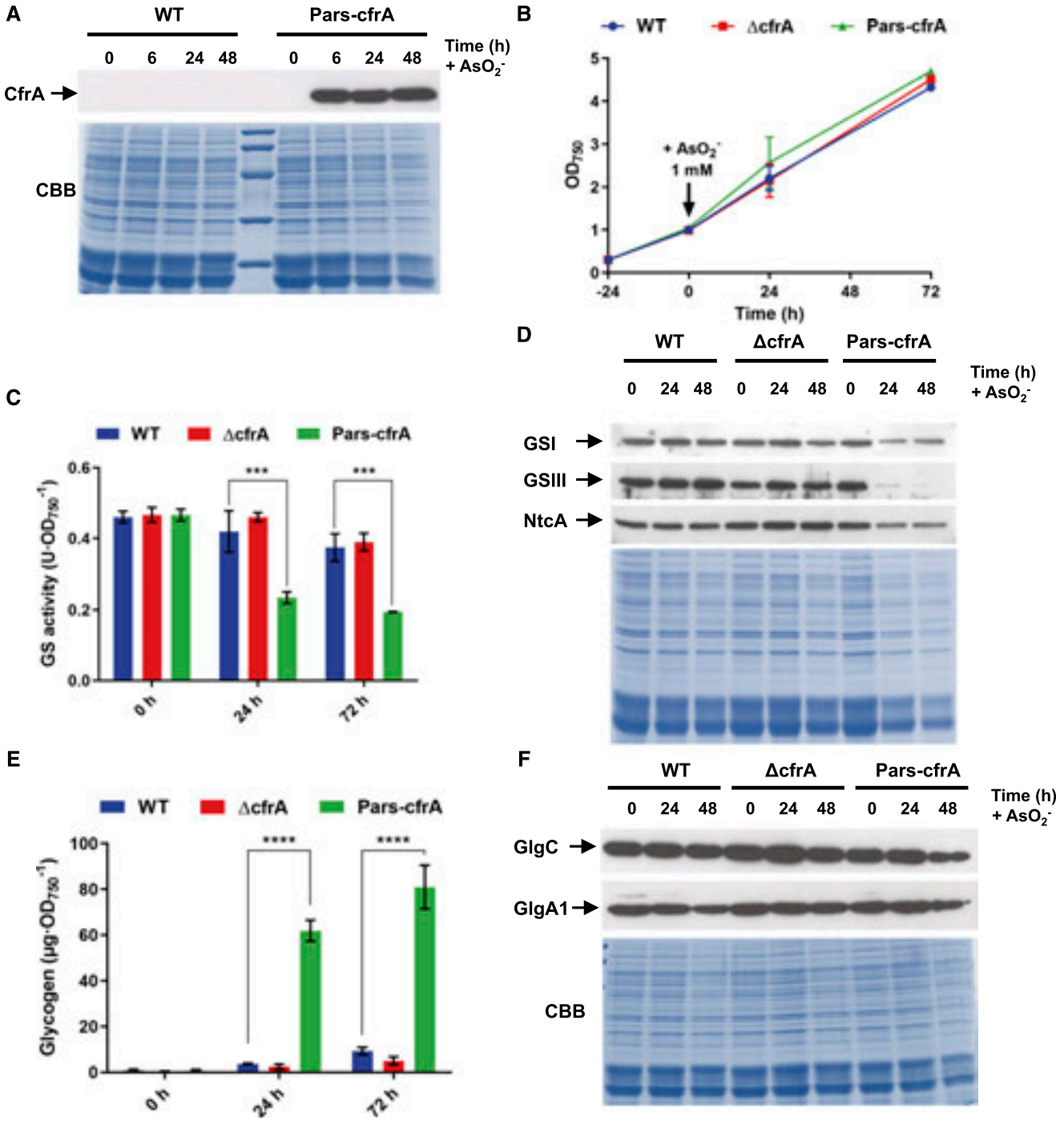

Figure 5. Comparative analysis of wild-type (WT), ΔcfrA, and Pars-cfrA strains. A, Western-blot analysis of CfrA in wild-type and Pars-cfrA strains at 0, 6, 24, and 48 h after 1 mM of arsenite addition. B, Growth analysis of wild-type, ΔcfrA, and Pars-cfrA before and after the addition of 1 mM of arsenite for CfrA overexpression. C, GS activity of wild-type, ΔcfrA, and Pars-cfrA at 0, 24, and 72 h after 1 mM of arsenite addition. D, Western-blot analysis of GSI, GSIII, and NtcA in wild-type, ΔcfrA, and Pars-cfrA strains at 0, 24, and 48 h after 1 mM of arsenite addition. E, Glycogen content of wild-type, ΔcfrA, and Pars-cfrA at 0, 24, and 72 h after 1 mM of arsenite addition. F, Western-blot analysis of GlgC and GlgA1 in wild-type, ΔcfrA, and Pars-cfrA strains at 0, 24, and 48 h after 1 mM of arsenite addition. In A, D, and F, total protein crude extracts were obtained from cells corresponding to 2 OD_{750} in every case. Equal volumes of each extract were loaded onto the gels, and Coomassie Brilliant Blue (CBB) staining is shown as a protein loading control. Error bars in B, C, and E represent SD of the mean values from three independent experiments. Asterisks indicate significance difference using ANOVA test (***$P = 0.0002$ and ****$P < 0.0001$).

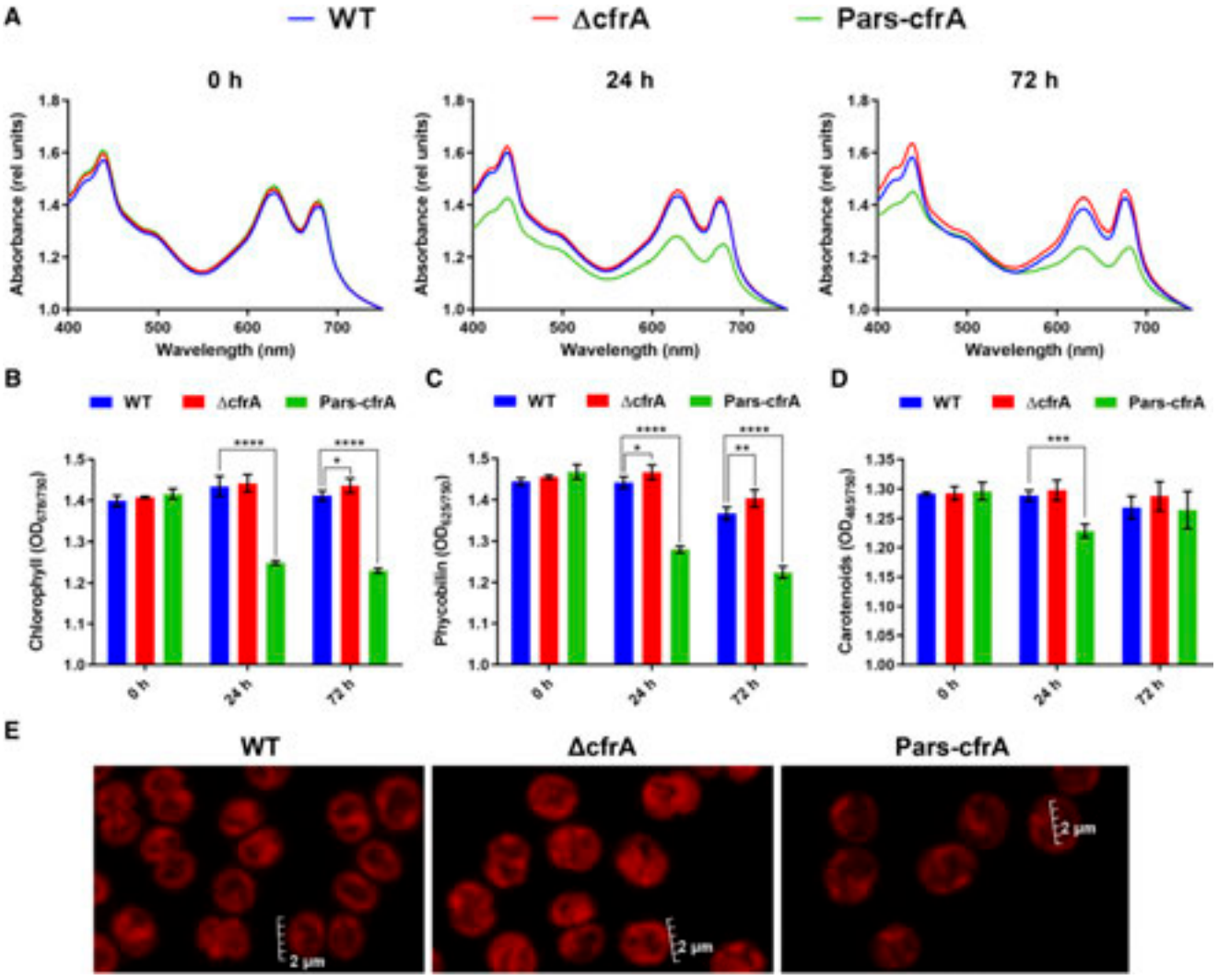

Figure 6. Photosynthetic pigments of wild-type (WT), ΔcfrA, and Pars-cfrA strains. A, Absorption spectra (400 to 750 nm) from wild-type, ΔcfrA, and Pars-cfrA strains before (0 h) and after (24 and 72 h) 1 mM of arsenite addition. Spectra were normalized to the same optical density at 750 nm of 1. B to D, Relative chlorophyll *a* (B), phycobilin (C), and carotenoid (D) contents in wild-type, ΔcfrA, and Pars-cfrA before (0 h) and after (24 h and 72 h) 1 mM of arsenite addition. E, Confocal microscopy autofluorescence images from wild-type, ΔcfrA, and Pars-cfrA 24 h after 1 mM of arsenite addition. Error bars in B to D represent SD of the mean values from three independent experiments. Asterisks indicate significance difference using ANOVA test (*$P < 0.05$, **$P < 0.005$, ***$P = 0.0001$, and ****$P < 0.0001$).

CfrA Overexpression Alters the Inner Structure and Morphology of *Synechocystis* Cells

As mentioned before, Pars-cfrA cultures showed slightly higher OD_{750} after arsenite addition than those of the wild-type or ΔcfrA strains (Fig. 5B; Supplemental Fig. S3A). We wondered whether these differences revealed faster growth of these cells or were instead due to changes in cell morphology or cell size. In addition, the decantation time of the cultures seemed to depend on the amount of CfrA, being shorter in the cultures of the Pars-cfrA strain compared to the wild type and slightly higher in the cultures of the ΔcfrA strain. (Supplemental Fig. S4).

We compared cells of the Pars-cfrA strain grown for 24 h in the presence or absence of arsenite using flow cytometry and could detect a small but significant increase in cell size and complexity of cells grown in the presence of arsenite. Again, a decrease in chlorophyll *a* content was associated to CfrA overexpression (Supplemental Fig. S5).

Cells of the wild-type, ΔcfrA, and Pars-cfrA strains were also analyzed using transmission electron microscopy to study the accumulation of storage compounds as well as the status of the cell cytoplasm and thylakoid membranes. As shown in Figure 8, and consistent with the results previously described, induction of CfrA expression in Pars-cfrA strain resulted in a high increase of glycogen accumulation, while the deletion of *cfrA* caused some decrease in glycogen content in

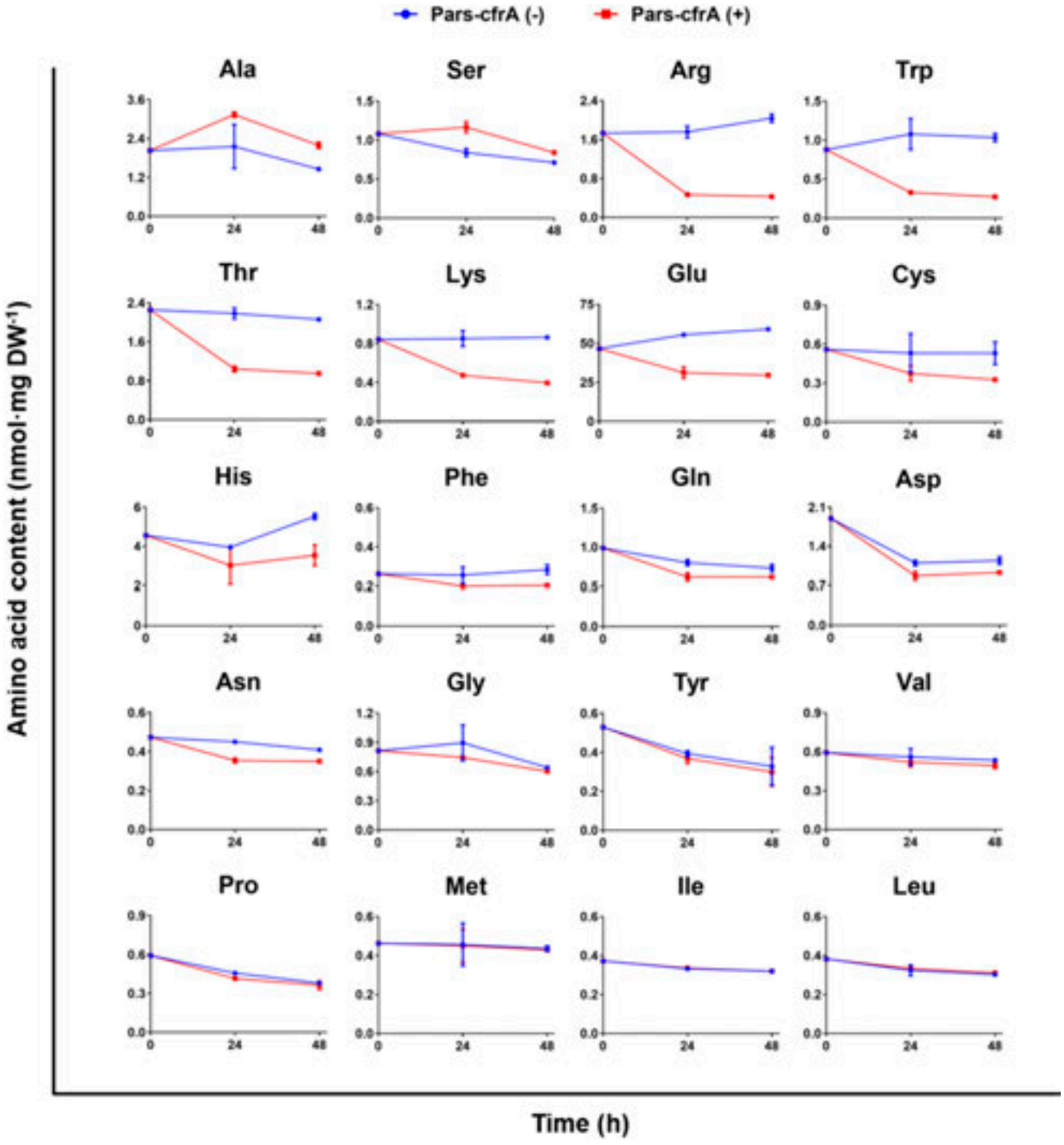

Figure 7. Amino acid pools analysis in Pars-cfrA strain. Evolution of amino acid pools in Pars-cfrA cells in the absence of arsenite (−) or in the presence of 1 mM of arsenite for the indicated time (+). Amino acid content (*y* axis) is specified in nmol per mg of dry weight (DW). Error bars represent SD of the mean values from four independent experiments.

comparison to the wild type. A significant but modest increase in glycogen content was observed in the cultures of the wild-type and ΔcfrA strains 24 h after the addition of arsenite. This increase is related to the age of the cultures and was quantified after 24 and 72 h of arsenite addition (Fig. 5E).

The Phenotype Associated with CfrA Overexpression Is Reversible

Considering the characteristics of the P_{arsB} promoter, the transcription of the *cfrA* gene in the Pars-cfrA strains would be stopped by removing the inducer. To analyze

the evolution of CfrA in the cultures upon arsenite removal, we proceeded as in previous experiments and after 72 h of arsenite addition, it was removed. The control culture was also washed to equalize the effects of biomass loss. Samples were collected for the analysis of cell growth, GS activity, chlorophyll, and glycogen content. As shown in Supplemental Figure S6, the phenotype associated with CfrA overexpression had reverted and CfrA was undetectable 72 h after removing the inducer.

CfrA Expression Levels Affect the Rate of Glycogen Consumption during the Reversal of Chlorosis

We compared glycogen accumulation levels of wild-type, ΔcfrA, and Pars-cfrA strains after addition of arsenite for 24 h and subsequent nitrogen starvation for 5 d. Evolution of this polymer during recovery of the chlorosis by nitrate addition was also analyzed, maintaining the presence of arsenite throughout the process. As shown in Figure 9A, the three strains accumulated high levels of glycogen under nitrogen starvation. This accumulation was only 10% lower in the knockout strain compared to the wild type, and 10% higher in the overexpressing strain. However, a clear difference could be observed in the mobilization of glycogen after the addition of nitrate to chlorotic cells. The knockout strain consumed glycogen faster than the wild-type strain, coinciding with its rapid regreening, while the Pars-cfrA strain showed a long delay in the reversal of chlorosis and a low mobilization of glycogen (Fig. 9).

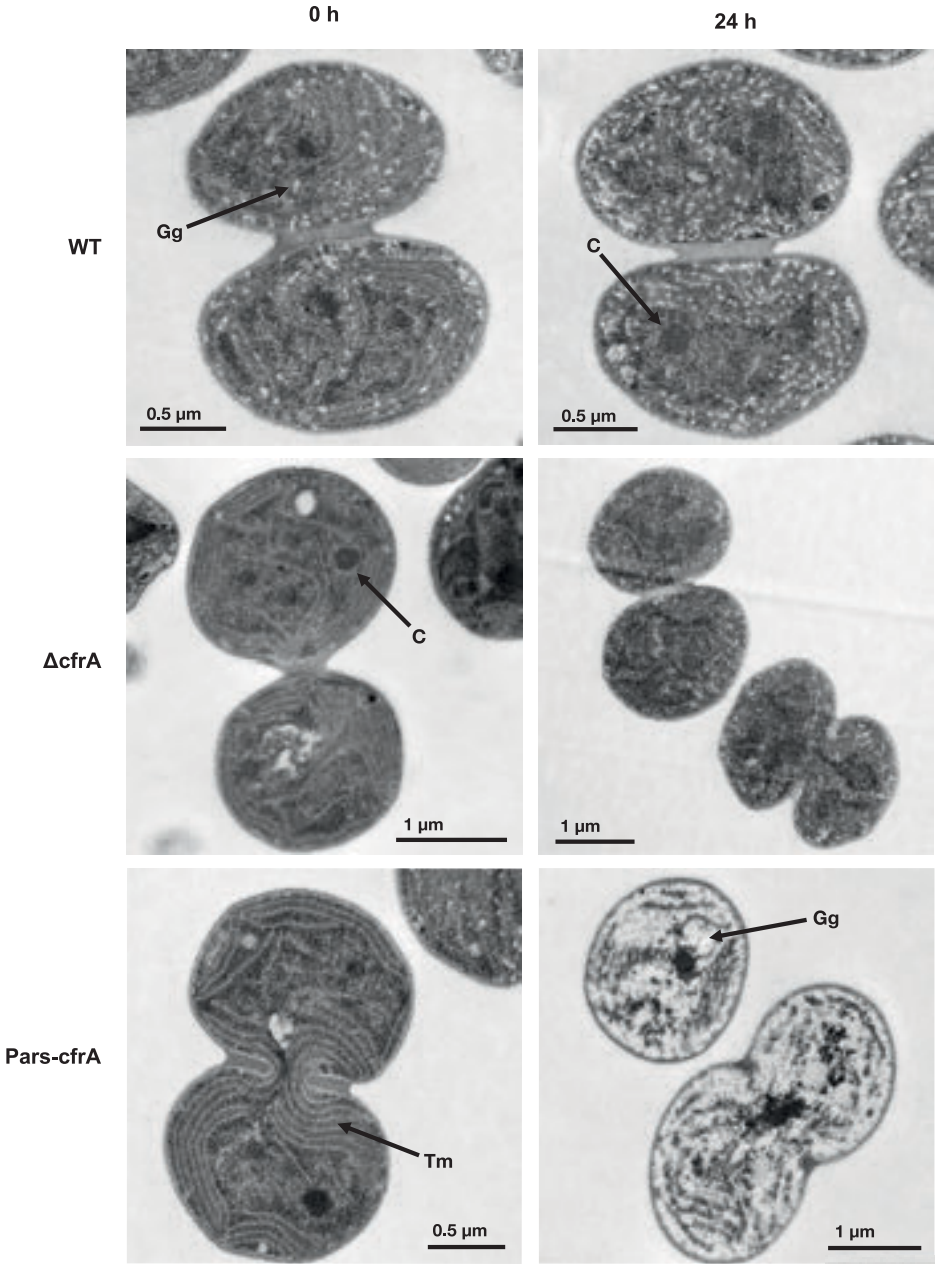

Figure 8. Electron microscopy images from wild-type (WT), ΔcfrA, and Pars-cfrA. Images were taken from samples before (0 h) and after 24-h growth with 1 mM of arsenite (24 h). C, Carboxysome; Gg, glycogen granules; Tm, Thylakoid membranes.

Various Components of the Pyruvate Dehydrogenase Complex and PII Protein Coimmunoprecipitated with CfrA

To identify possible CfrA interactors, cells of the Pars-cfrA strain cultivated in the presence of arsenite for 24 h were used to obtain crude extracts. CfrA was immunoprecipitated using anti-CfrA antibodies coupled to protein-A superparamagnetic beads. A control with preimmune serum was carried out in parallel. Precipitated material in both cases was analyzed by liquid chromatography with tandem mass spectrometry (LC-MS/MS) using a time-of-flight quadrupole and the software ProteinPilot v5.0.1 (Sciex) for protein identification (Supplemental Methods S2). A list of the proteins identified ordered by their score, based on the number of distinctive peptides identified and the false discovery rate, is available (Supplemental Dataset S2). One of the proteins identified only with the immune serum with highest score was dihydrolipoamide dehydrogenase, a component of the pyruvate dehydrogenase (PDH) complex and other 2-oxo acid dehydrogenase complexes (Engels and Pistorius, 1997). Interestingly, two other specific components of the PDH complex also coimmunoprecipitated with CfrA, dihydrolipoamide acetyltransferase, and pyruvate dehydrogenase E1 beta subunit. These results point to an interaction of CfrA with the PDH complex that could modulate its activity, thus regulating the flow of carbon toward the tricarboxylic acid cycle. The signal transduction PII protein was also identified in the immunoprecipitation with anti-CfrA serum. The fact that this protein is a regulator of the C/N homeostasis prompted us to further investigate their relationship with CfrA. Additionally, in the course of this work the presence of CfrA in pull-down experiments using PII-FLAG protein was reported (Watzer et al., 2019).

Overexpression of CfrA Causes High Glycogen Accumulation Irrespective of the Presence of PII

To study if the phenotype associated with CfrA overexpression was somehow dependent on PII, the *cfrA* version controlled by P_{arsB} was introduced in a strain lacking PII (ΔglnB). The resulting strain, ΔglnB/Pars-cfrA, was analyzed together with its parental strain ΔglnB. The Pars-cfrA strain was included as a control of CfrA expression and glycogen accumulation. Comparative phenotypic analysis in an induction experiment with arsenite is shown in Figure 10. Addition of arsenite to ΔglnB/Pars-cfrA strain stopped growth of this strain in ~24 h, indicating that overexpression of CfrA in the absence of PII is lethal under the conditions tested (Fig. 10A). Accumulation of CfrA 24 and 48 h after arsenite addition was considerably lower in the ΔglnB/Pars-cfrA strain compared to the Pars-cfrA strain (Fig. 10B). PII protein was also analyzed to verify the ΔglnB strain as well as to test whether the overexpression of CfrA in the Pars-cfrA strain entails any modification in PII accumulation. A slight increase in the amount of PII could be observed in the Pars-cfrA strain after the addition of arsenite (Fig. 10B). This increase did not take place in the wild type, so it cannot be attributed to the addition of arsenite (not shown). Similar to strains with an intact *glnB locus*, CfrA overexpression in a Δ*glnB* genetic background leads to a decrease in the total protein content as well as in the activity and amount of GS, but these effects were somewhat more drastic than those described in strains with PII (Fig. 10, B and C). With respect to glycogen, accumulation of this polymer dependent on the addition of arsenite was observed in both strains, ΔglnB/Pars-cfrA and Pars-cfrA, but this accumulation was significantly higher in the ΔglnB/Pars-cfrA strain (Fig. 10D). As in Pars-cfrA strain, overexpression of CfrA in a Δ*glnB* genetic background caused a decrease in photosynthetic pigments (Fig. 10E).

DISCUSSION

Glycogen is the main carbon sink in cyanobacteria, and adaptation to nitrogen deficiency in nondiazotrophic cyanobacteria requires correct glycogen metabolism. In fact, mutants defective in glycogen synthesis are unable to acclimate and survive the nitrogen starvation (Gründel et al., 2012). Our results indicate that the CfrA protein begins to accumulate in *Synechocystis* early after the removal of the nitrogen source (Fig. 2), and that this accumulation is maintained at high levels during the first 48 h of nitrogen starvation. This period matches the early response to nitrogen deficiency in which the progression of chlorosis and glycogen synthesis take place simultaneously (Krasikov et al., 2012; Klotz et al., 2016). Consistent with this expression pattern, the analysis of strains with different amounts of CfrA shows that the amount of glycogen that accumulates in cells clearly depends on the quantity of CfrA, even if the protein is expressed independently of the nitrogen conditions (Figs. 4C, 5E, and 8). These results indicate that CfrA controls the amount of carbon stored as reserve, supporting the hypothesis that CfrA is involved in redirection of the carbon excess toward glycogen synthesis under conditions of nitrogen starvation.

As shown in Figure 2, the amount of CfrA reaches minimum levels in both the wild-type and the Ptrc-cfrA strains after a prolonged period of nitrogen deficiency. This corresponds to a state of fully developed chlorosis in which the translational machinery must be reduced to the minimum. The transitory increase in CfrA accumulation after readdition of nitrate could correspond to the translation of pre-existing *cfrA* transcripts because an increase in mRNA stability in chlorotic cells has been proposed (Klotz et al., 2016). Interestingly, this period coincides with the reported first resuscitation phase of chlorotic cells, energetically supported by respiration and before the de novo synthesis of the photosynthetic machinery (Klotz et al., 2016).

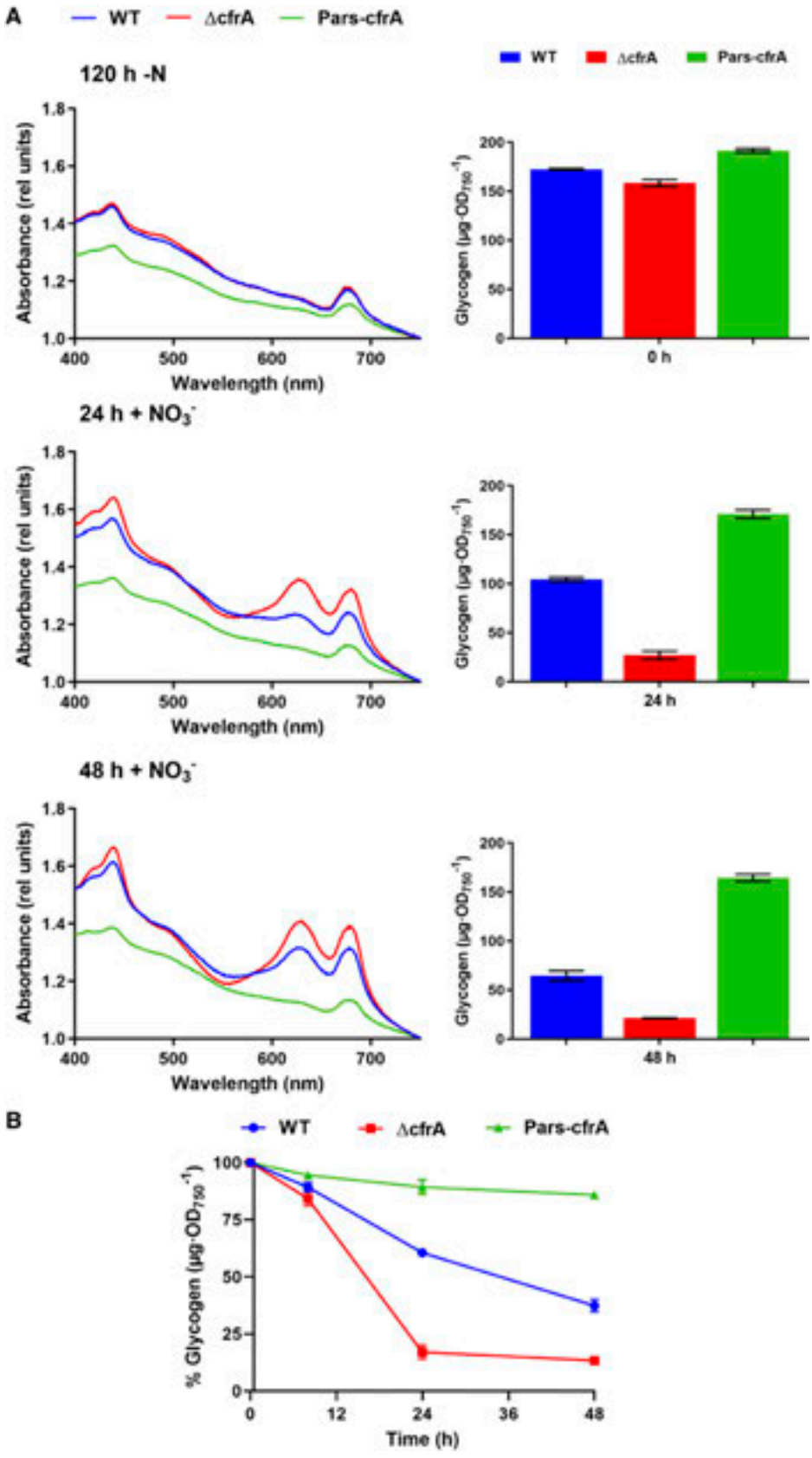

Figure 9. Glycogen consumption and evolution of pigments during the reversal of chlorosis. A, Absorption spectra (400 to 750 nm) and glycogen content of *Synechocystis* cultures from wild-type (WT), ΔcfrA, and Ptrc-cfrA strains during the reversal of chlorosis. After 5 d of nitrogen starvation (120 h −N), sodium nitrate (17.6 mM) was added to cultures and spectra were performed at the indicated times (+ NO_3^-). Spectra were normalized to the same optical density at 750 nm of 1. On the right, the glycogen accumulated by each strain at each stage of the process is shown. B, Evolution of relative glycogen content with respect to that of chlorotic cells. The glycogen content of each strain is shown during the reversal of chlorosis relative to the accumulated amount before the addition of nitrate (100%). Error bars represent SD of the mean values from two independent experiments.

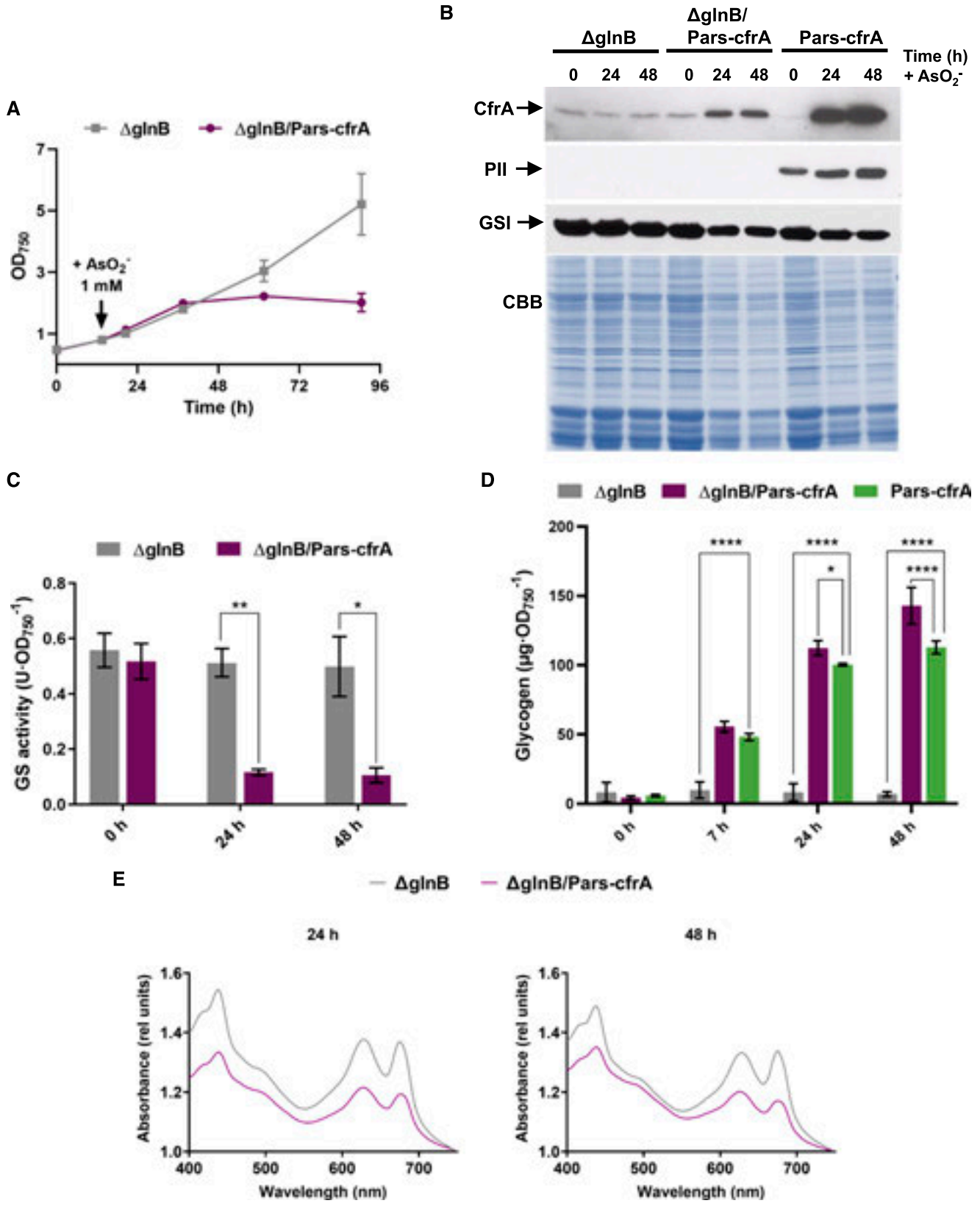

Figure 10. Comparative analysis of ΔglnB, ΔglnB/Pars-cfrA, and Pars-cfrA strains. A, Growth analysis of ΔglnB and ΔglnB/Pars-cfrA before and after the addition of 1 mM of arsenite for CfrA overexpression. B, Western-blot analysis of CfrA, PII, and GSI in ΔglnB, ΔglnB/Pars-cfrA, and Pars-CfrA strains at 0, 24, and 48 h after 1 mM of arsenite addition. Total protein crude extracts were

The delay in the chlorosis reversion observed in the Ptrc-cfrA and Pars-cfrA strains (Figs. 3 and 9; Supplemental Fig. S2) could indicate that the presence of high levels of CfrA during the awakening process would partially prevent the flow of carbon toward protein synthesis, thus delaying the reconstitution of the photosynthetic apparatus and the recovery as a whole. In line with this, the strain lacking CfrA presents a faster reversal of chlorosis with respect to the wild-type strain, and rapidly mobilizes the glycogen accumulated in the period of nitrogen deficiency (Fig. 9).

The accumulation of glycogen depends on the amount of carbon available, which is a function of the availability of light and CO_2 or an extra source such as Glc (Zavřel et al., 2017). Accordingly, the observed glycogen accumulation in the Pars-cfrA strain was dependent on carbon supply. This can be seen by comparing the cultures in BG11C (Fig. 4C) with those made in BG11C supplemented with CO_2 (Fig. 5E). With similar levels of CfrA, the amount of accumulated glycogen was greater under conditions of higher carbon availability. These results confirm that it is the photosynthetic capacity that ultimately controls the global carbon flux.

Some studies in *Synechocystis* have linked a higher content of glycogen with larger cell size (Yamauchi et al., 2011; Zavřel et al., 2017). Accordingly, the slight increase in size observed in the Pars-cfrA strains (Fig. 6E; Supplemental Fig. S5) and their faster decantation (Supplemental Fig. S4) could be related to their glycogen content.

A remarkable phenotypic feature associated with the induction of CfrA expression in Pars-cfrA strains was the decrease in photosynthetic pigments (Figs. 6 and 10E; Supplemental Fig. S3F). This partial chlorosis took place under conditions of nitrogen sufficiency and is different from that associated with the chlorotic response to nitrogen starvation, because it did not imply the characteristic almost-complete loss of the photosynthetic apparatus. Our hypothesis is that the overexpression of CfrA causes a decrease in carbon flux toward the tricarboxylic acid cycle and therefore toward the production of carbon skeletons for protein synthesis, namely 2-OG. A decrease in total protein synthesis results in a progressive loss of the content of phycobiliproteins with the consequent change in the coloration of the culture as growth progresses. This decrease in the amount of total protein could be observed in the crude extracts of the strain Pars-cfrA analyzed by SDS-PAGE and Coomassie staining (Figs. 5, A, D, and F, and 10B). Accordingly, the ΔcfrA strain presented a slight but significantly greater quantity of phycobilins with respect to the wild type (Fig. 6C), consistent with the small difference in the amount of CfrA between these two strains under conditions of nitrogen sufficiency. As occurs in the Pars-cfrA strains, a reduced amount of photosynthetic pigments is associated with a higher amount of glycogen in other *Synechocystis* strains, as is the case of CyAbrB mutants (Yamauchi et al., 2011).

If CfrA overexpression leads to much of the assimilated carbon being destined for the synthesis of glycogen to the detriment of its use for anabolic processes, the assimilation of nitrogen through the GS-GOGAT cycle should decrease with this overexpression. In fact, a decrease in GS activity could always be observed when the amount of CfrA increases (Figs. 4D, 5C, and 10C; Supplemental Figs. S3D and S6C). Several factors could contribute to this downregulation of the GS activity. Low levels of 2-OG would have a double effect, decreasing the transcription of the *glnA*, *glnN*, and *ntcA* genes (activated by NtcA depending on the concentration of 2-OG; Giner-Lamia et al., 2017) and decreasing nitrogen assimilation and general protein synthesis as a substrate of the GS-GOGAT cycle. A decrease in the amount of GSI, GSIII, and NtcA was associated with overexpression of CfrA (Fig. 5D).

The expected direct consequence of a decrease in the activity of the GS-GOGAT cycle would be the decrease in its product Glu, which is by far the most abundant amino acid in *Synechocystis* (Kiyota et al., 2014) and the major source of nitrogen for cellular metabolism (Flores and Herrero, 2004). As shown in Figure 7, the intracellular Glu pool decreased significantly (~50%) in the Pars-cfrA strain when CfrA expression was induced. This reduction resulted also in a drastic decrease in the Arg pool, an amino acid synthesized from Glu, which is a nitrogen reservoir. The levels of other amino acids were also reduced, to a greater or lesser extent, with CfrA overexpression. The synthesis of most of these amino acids involves the participation of Glu or Gln as donors of the amino group, and therefore their homeostasis will be influenced by the intracellular level of these nitrogen distributors. Interestingly, the amounts of several of these amino acids (Glu, Gln, Arg, Asp, Trp, and Asn) also decrease during early acclimation to nitrogen starvation, conditions in which CfrA is naturally expressed and protein synthesis is limited by the absence of nitrogen. Also, in agreement with what happens under nitrogen deficiency (Kiyota et al., 2014;

Figure 10. (*Continued.*)
obtained from cells corresponding to 2 OD_{750} in every case. Equal volumes of each extract were loaded, and Coomassie Brilliant Blue (CBB) staining is shown as protein loading control. C, GS activity of ΔglnB and ΔglnB/Pars-cfrA strains at 0, 24, and 48 h after 1 mM of arsenite addition. Asterisks indicate significance difference using multiple *t* test (*$P \leq 0.1234$ and **$P \leq 0.0021$). D, Glycogen content of ΔglnB, ΔglnB/Pars-cfrA, and Pars-CfrA at 0, 24, and 48 h after 1 mM of arsenite addition. Asterisks indicate significance difference using ANOVA test (*$P < 0.05$ and ****$P < 0.0001$). E, Absorption spectra (400 to 750 nm) from ΔglnB and ΔglnB/Pars-cfrA strains after 24 or 48 h of 1 mM of arsenite addition. Error bars in A, C, and D represent SD of the mean values from three independent experiments.

Osanai et al., 2014b), some amino acids synthesized from pyruvate or 3-phosphoglycerate (Ala and Ser) experienced a moderate increase with the overexpression of CfrA (Fig. 7). These data lead us to propose that CfrA could limit the carbon flow toward acetyl-CoA synthesis during adaptation to nitrogen limitation, increasing the amount of some glycolytic intermediates and redirecting the flow toward glycogen synthesis while decreasing the flow toward tricarboxylic acid cycle and protein synthesis (Fig. 11). The identification of various components of the PDH complex as possible CfrA interactors (Supplemental Dataset S2) suggests that it could modulate the activity of this complex, which would agree well with the hypothesis. In line with this, studies of metabolic flux changes under nitrogen starvation demonstrated minimal flux into acetyl-CoA via PDH in these conditions (Qian et al., 2018). In fact, a large-scale study of protein–protein interaction identified a possible interaction between *sll0944* ORF and the E1 subunit of the PDH complex (Sato et al., 2007).

Our results, along with others recently published (Watzer et al., 2019), show that the PII regulatory protein also interacts with CfrA. Accumulation of CfrA from the P_{arsB} promoter in the PII-deficient strain ΔglnB/Pars-cfrA was lower than that observed in the Pars-cfrA strain. An effect of PII deficiency on P_{arsB} activity is not expected, but rather we hypothesized a stabilizing effect of PII on CfrA perhaps mediated by their interaction. Accordingly, a slight increase of PII was observed in the Pars-cfrA strain by inducing CfrA expression. Interestingly, although the PII protein is very abundant (Forcada-Nadal et al., 2018), its expression increases in conditions of nitrogen deficiency (Giner-Lamia et al., 2017), in which CfrA is physiologically expressed. These results could indicate a possible buffering or modulating role of PII on CfrA activity. In this sense, in the absence of PII, the action of CfrA would be enhanced.

Regarding the lethality of CfrA overexpression in the absence of PII under conditions of nitrogen sufficiency, some hypotheses can be raised. The PII protein has been described to interact with acetyl-CoA carboxylase (ACCase), negatively regulating fatty acid synthesis based on available carbon. This interaction is inhibited by 2-OG in a dose-dependent manner (Hauf et al., 2016). It has been proposed that PII, by controlling ACCase, could modulate the distribution of the carbon flux toward either the tricarboxylic acid cycle and GS-GOGAT cycle or toward lipid biosynthesis (Forchhammer and Selim, 2020). In addition, the interaction of the PII protein with phosphoenol pyruvate carboxylase (PEPC), an enzyme that plays an important role in the flow of carbon to the tricarboxylic acid cycle, has recently been reported. This interaction increases the PEPC activity and therefore the oxaloacetate synthesis when the 2-OG concentration is low (Scholl et al., 2020). The overexpression of CfrA, which leads to a decrease in the carbon flux toward 2-OG (probably acting on PDH), in a genetic background lacking PII and therefore without the negative control of the ACCase and the positive action on PEPC, could

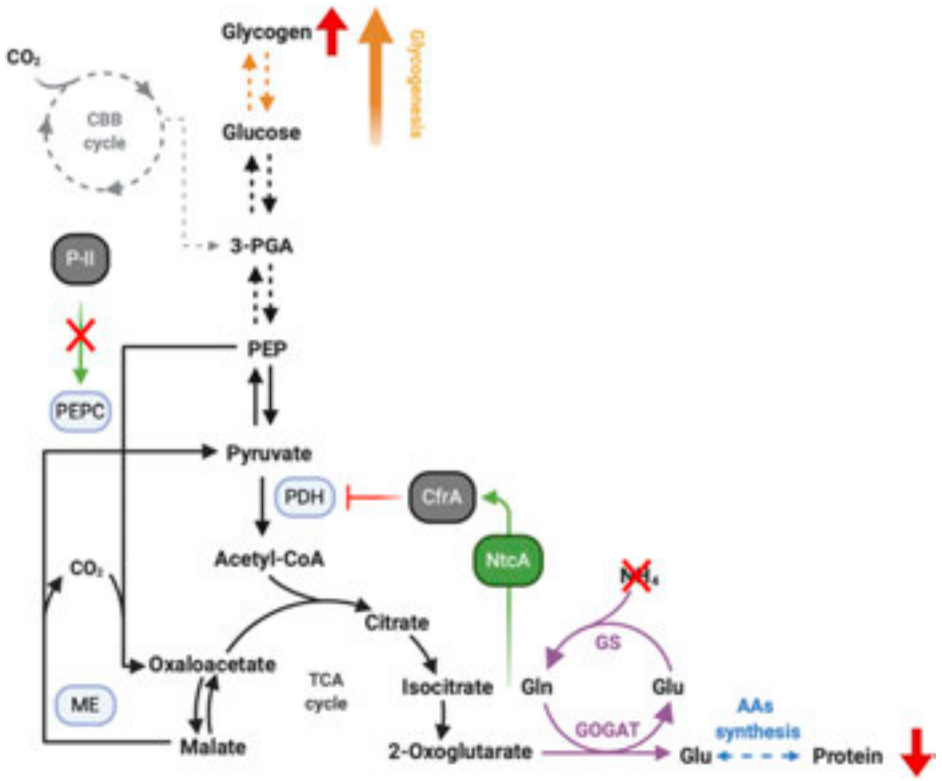

Figure 11. Schematic model of CfrA action under nitrogen starvation. 2-OG, the substrate of the GS-GOGAT cycle, accumulates in the absence of a nitrogen source. The resulting imbalance activates NtcA, which will induce the expression of CfrA. This latter would reduce the flow of carbon to the tricarboxylic acid cycle, probably acting at the PDH level. In such situation, the high levels of 2-OG would also prevent the described positive effect of the PII protein on PEPC activity (Scholl et al., 2020), contributing to a reduction of tricarboxylic acid cycle intermediates. Overall, this leads to a protein synthesis limitation and the net carbon flux redirection toward glycogen synthesis. CBB cycle, Calvin–Benson–Bassham cycle; ME, malic enzyme.

lead to the observed lethality of the ΔglnB/Pars-cfrA strains by depletion of the 2-OG and Glu pools. In fact, PII-deficient mutants have been reported to have greatly reduced levels of 2-OG and Glu (Schwarz et al., 2014; Scholl et al., 2020). Our data indicate that CfrA overexpression also causes a considerable reduction in the Glu pool (Fig. 7). The combination of both effects could have lethal consequences.

In the proposed model for the wild-type strain under nitrogen limitation (high 2-OG), both CfrA and PII would contribute to reduce flow to the tricarboxylic acid cycle and 2-OG synthesis via its control of PDH (inhibition) and PEPC (absence of activation), respectively (Fig. 11). However, understanding the mechanistic details and metabolic consequences of the functional relationship among CfrA, PDH, and PII requires further investigation, as well as some other possible interactions of CfrA (Supplemental Dataset S2).

A deeper knowledge of metabolic circuits is needed to successfully address different biotechnological strategies in cyanobacteria. Carbon metabolism and its plasticity are key points of interest to redirect the fixed CO_2 toward the synthesis of valuable compounds (Xiong et al., 2017). Due to the advantages of glycogen over lignocellulosic biomass (Möllers et al., 2014), the possible development and use of cyanobacterial strains with high glycogen content has been considered on several occasions (Shimakawa et al., 2014; Gupta et al., 2020). Pars-cfrA strains have a high potential in biomass production due to the large amount of glycogen they accumulate compared to the wild type (Figs. 5E and 10D). Furthermore, this accumulation, unlike what occurs in the wild type, takes place in the presence of a nitrogen source in stably growing cultures.

MATERIALS AND METHODS

Culture Conditions

Synechocystis sp. PCC 6803 derivative strains were grown photoautotrophically at 30°C on BG11 medium (Rippka, 1988), supplemented with 1 g L^{-1} $NaHCO_3$ (BG11C) and bubbled with 1% (v/v) CO_2 in air, under continuous illumination (50 to 70 μmol of photons m^{-2} s^{-1}; 4000 K LED lights), hereafter used as "standard" conditions. Nitrogen deficiency was induced by removal of combined nitrogen. For plate cultures, 1% (w/v) Bacto agar (Difco) and the required antibiotics were added (50 μg mL^{-1} of kanamycin, 2.5 μg mL^{-1} of spectinomycin, 2.5 μg mL^{-1} of streptomycin, and 20 μg mL^{-1} of chloramphenicol). Sodium arsenite ($NaAsO_2$) at different concentrations was added when required. Growth was monitored via optical density at 750 nm (OD_{750}). Chlorophyll concentration was determined in methanolic extracts (Mackinney, 1941). Total protein concentration was determined as described in Lowry et al. (1951).

Generation of Mutant Strains of *Synechocystis*

To generate the ΔcfrA strain, 1,149- and 962-bp DNA fragments were amplified from genomic DNA by PCR using the oligonucleotides cfrA1F and cfrA1R or cfrA2F and cfrA2R, respectively. Those fragments were combined by PCR to generate a 2,081-bp fragment containing the *cfrA locus* with the CfrA coding sequence deleted. This fragment was cloned into pSparkII (Canvax). An Sm^r Sp^r C.S3 cassette (Prentki and Krisch, 1984) from pRL463 (Elhai and Wolk, 1988) was cloned in the *Bst*EII site of *cfrA locus* generating plasmid pΔcfrA, which was introduced in the wild-type strain (Supplemental Fig. S1).

To generate Ptrc-cfrA strain, a DNA fragment containing *cfrA* was amplified by PCR using genomic DNA and oligonucleotides cfrANco and cfrASma. This fragment was cloned into *Nco*I-*Sma*I digested pTrc99A (Amann et al., 1988). An *Eco*RV-*Sma*I fragment from the resulting plasmid containing the P_{trc} promoter, a ribosome binding site from pTrc99A, and the *cfrA* ORF, was cloned into *Sma*I-digested pPLAT plasmid (Galmozzi et al., 2007) containing a 2-kb region of the nonessential *nrsBACD* operon (García-Domínguez et al., 2000). Finally, a Km^r CK1 cassette from pRL161 (Elhai and Wolk, 1988) was cloned in the *Bam*HI site of pPLAT. This plasmid was used to transform the ΔcfrA strain (Supplemental Fig. S1).

To generate the Pars-cfrA strain, a DNA fragment containing *cfrA* and a ribosome binding site was amplified by PCR from pET24-CfrA (a pET24 derivative described in Supplemental Methods S1), using oligonucleotides cfrApETXba and cfrAXhoArs. This fragment was cloned into *Xba*I-*Xho*I–digested parsBnrsD plasmid, which contains a synthetic polylinker that allows cloning and expression of genes under the regulation of P_{arsB} promoter, and the sequence for homologous recombination in the nonessential *nrsD locus* (García-Domínguez et al., 2000). A Km^r CK1 cassette from pRL161 (Elhai and Wolk, 1988) was cloned in the *Hin*dIII site of parsBnrsD. This plasmid (parsBnrsDcfrA) was used to transform the ΔcfrA strain (Supplemental Fig. S1).

To generate the ΔglnB strain, 903- and 904-bp DNA fragments were amplified from genomic DNA by PCR using the oligonucleotides glnBEcoRV and glnBR or glnBNot and glnBF, respectively. Those fragments were combined by PCR to generate a 1,771-bp fragment containing the *glnB locus* with most of the PII-coding sequence deleted and replaced by a *Bam*HI site. This fragment, *Eco*RV-*Not*I–digested, was cloned into pBS KS(+) plasmid digested with the same enzymes. A Cm^r C.C1 cassette from pRL171 (Elhai and Wolk, 1988) was cloned in the *Bam*HI site generating plasmid pΔglnB, which was introduced in the wild-type strain.

All DNA constructs and strains were verified by DNA sequencing and PCR analysis. Oligonucleotides used are summarized in Supplemental Table S1. *Synechocystis* strains used in this work are stated in Table 1.

Preparation of Crude Extracts and Western-Blot Analysis

For the analysis of proteins abundance, 2 U OD_{750} were harvested and resuspended in 80 μL of 50-mM HEPES-NaOH buffer (pH 7.0), 50 mM of KCl, and 1 mM of phenylmethylsulfonyl fluoride. Crude extracts were prepared using glass beads as described in Reyes et al. (1995). For western-blot analysis, proteins were fractionated on 12% (w/v) SDS-PAGE (Laemmli, 1970) and transferred to nitrocellulose membranes (Bio-Rad). Blots were blocked with 5% (w/v) nonfat dry milk (AppliChem) in phosphate-buffered saline-TWEEN 20. Antisera were used at the following dilutions: Anti-CfrA (1:10,000; Supplemental Methods S1), anti-GSI (1:250,000; Marqués et al., 1992), anti-GSIII (1:10,000; García-Domínguez et al., 1997), anti-NtcA (1:2,000; Giner-Lamia et al., 2017), anti-PII (1:4,000; Giner-Lamia et al., 2017), anti-GlgC and anti-GlgA1 (1:10,000 and 1:5,000, respectively; Díaz-Troya et al., 2014). The ECL Prime Western Blotting Detection Reagent (GE Healthcare) was used to detect the different antigens with anti-rabbit secondary antibodies (1:25,000; Sigma-Aldrich). In all cases, at least three independent experiments were carried out and a representative western-blot is shown.

GS Assay

GS activity was determined in situ by using the Mn^{2+}-dependent γ-glutamyltransferase assay in permeabilized cells (Mérida et al., 1991).

Photosynthetic Pigment Analysis

Absorption spectra (400 to 750 nm) of *Synechocystis* cultures were measured and peaks at 485, 625, and 678 nm were used for carotenoid, phycobilin, and chlorophyll content analysis, respectively. All spectra were normalized to 1 OD_{750} for the comparison of different samples. Autofluorescence was detected by laser confocal microscopy (FLUOVIEW FV 3000; Olympus) using the 488-nm line supplied by an argon ion laser. Fluorescent emission was monitored by collection across a window of 630 to 700 nm.

Glycogen Content Determination

Glycogen was determined as described in Xu et al. (2013) with some modifications. Two units of OD_{750} were harvested, washed twice with Milli-Q water (EMD Millipore), and resuspended in 300 μL of 30 mM of sodium acetate at pH 5.2. Cells were disrupted with glass beads (0.15 to 0.25 mm) in a beadbeater, and the extract was recovered and boiled for 20 min. Two 100-μL aliquots were prepared; one of them was treated with 10 U amyloglucosidase from *Aspergillus niger* (Sigma-Aldrich) and the other with water as a control, incubating at 55°C overnight. Alternatively, glycogen was extracted as described in Klotz et al. (2016) and digested with amyloglucosidase under these same conditions. A calibration curve using commercial glycogen was also prepared. Released Glc was determined in all samples by the Glc oxidase/peroxidase method (cat. no. GAGO-20; Sigma-Aldrich). In all the glycogen determinations, two technical replications of each independent biological sample were carried out.

Amino Acid Pools Quantification

Amino acid pools were quantified by reverse-phase high performance liquid chromatography (Heinrikson and Meredith, 1984). Cells were harvested and lyophilized. Twenty milligrams of dry weight were resuspended in 400 μL of 0.1 M of HCl. After centrifugation to remove cell debris, 60-μL samples were derivatized by the Pico-Tag system (Waters; ethanol/water/triethylamine/phenylisothiocyanate, 7:1:1:1), dried and resuspended in diluent (2 M of Na_2PO_4, 10% [v/v] H_3PO_4, and 5% [v/v] acetonitrile). The separation was carried out with a 100 RP-18 LiChrospher column (Merck) using 5 μm of KgaA. Amino acids were detected by absorbance and quantified using standards of known concentration.

Electron Microscopy

Cells were fixed for 2 h at 25°C using 2.5% (w/v) glutaraldehyde in Na-cacodylate buffer (0.1 M at pH 7.4), washed five times with the same buffer at 25°C and incubated for 1 h at 4°C in the same buffer containing 1% (w/v) osmium tetroxide. Cells were then washed, immersed in 2% (w/v) uranyl acetate, dehydrated using serial concentrations of acetone (50, 70, 90 and 100% [v/v]), and finally embedded in Spurr resin. Three-hundred–nanometer sections were obtained and stained with 1% toluidine blue to orient and locate the cells in the samples using optical microscopy. Ultra-thin sections (70 nm), obtained using an ultramicrotome (model no. UC7; Leica) with diamond blade, and were placed on 200-mesh copper grids. All samples were analyzed in a Libra 120 Transmission Electron Microscope (Zeiss) and digital images were obtained using an on-axis mounted TRS camera.

Accession Numbers

The accession numbers of the proteins with the DUF1830 domain and the proteins identified in the immunoprecipitation assays are indicated in Supplemental Datasets S1 and S2, respectively.

Supplemental Data

The following supplemental materials are available.

Supplemental Figure S1. Scheme of gene structure of different CfrA *Synechocystis* strains.

Supplemental Figure S2. Pigmentation of *Synechocystis* cells with different levels of CfrA during resuscitation of chlorosis.

Supplemental Figure S3. Analysis of Pars-cfrA strain.

Supplemental Figure S4. Decantation of wild-type, ΔcfrA, and Pars-cfrA cells in BG11C medium.

Supplemental Figure S5. Flow cytometry characterization of Pars-cfrA strain.

Supplemental Figure S6. Phenotypic analysis of the Pars-cfrA strain after the removal of arsenite.

Supplemental Table S1. List and sequence of oligonucleotides used in this work.

Supplemental Dataset S1. Compilation of DUF1830-domain–containing sequences.

Supplemental Dataset S2. List of protein identified by LC-MS/MS in immunoprecipitation assays.

Supplemental Methods S1. CfrA-His_6 expression and purification and anti-CfrA antibody production.

Supplemental Methods S2. Immunoprecipitation assay and LC-MS/MS protein identification.

ACKNOWLEDGMENTS

We thank Dr. Luis López-Maury for parsBnrsD plasmid and Dr. Alicia M. Muro-Pastor for a critical reading of the article.

Received August 7, 2020; accepted August 22, 2020; published September 8, 2020.

LITERATURE CITED

Amann E, Ochs B, Abel KJ (1988) Tightly regulated tac promoter vectors useful for the expression of unfused and fused proteins in *Escherichia coli*. Gene **69:** 301–315

Angermayr SA, Hellingwerf KJ, Lindblad P, de Mattos MJ (2009) Energy biotechnology with cyanobacteria. Curr Opin Biotechnol **20:** 257–263

Berla BM, Saha R, Immethun CM, Maranas CD, Moon TS, Pakrasi HB (2013) Synthetic biology of cyanobacteria: Unique challenges and opportunities. Front Microbiol **4:** 246

Bolay P, Muro-Pastor MI, Florencio FJ, Klähn S (2018) The distinctive regulation of cyanobacterial glutamine synthetase. Life (Basel) **8:** 52

Carrieri D, Lombardi T, Paddock T, Cano M, Goodney GA, Nag A, Old W, Maness P-C, Seibert M, Ghirardi M, et al (2017) Transcriptome and proteome analysis of nitrogen starvation responses in *Synechocystis* 6803 ΔglgC, a mutant incapable of glycogen storage. Algal Res **21:** 64–75

Choi SY, Park B, Choi IG, Sim SJ, Lee SM, Um Y, Woo HM (2016) Transcriptome landscape of *Synechococcus elongatus* PCC 7942 for nitrogen starvation responses using RNA-seq. Sci Rep **6:** 30584

Crooks GE, Hon G, Chandonia JM, Brenner SE (2004) WebLogo: A sequence logo generator. Genome Res **14:** 1188–1190

Díaz-Troya S, López-Maury L, Sánchez-Riego AM, Roldán M, Florencio FJ (2014) Redox regulation of glycogen biosynthesis in the cyanobacterium *Synechocystis* sp. PCC 6803: Analysis of the AGP and glycogen synthases. Mol Plant **7:** 87–100

Elhai J, Wolk CP (1988) A versatile class of positive-selection vectors based on the nonviability of palindrome-containing plasmids that allows cloning into long polylinkers. Gene **68:** 119–138

Engels A, Pistorius EK (1997) Characterization of a gene encoding dihydrolipoamide dehydrogenase of the cyanobacterium *Synechocystis* sp. strain PCC 6803. Microbiology (Reading) **143:** 3543–3553

Esteves-Ferreira AA, Inaba M, Fort A, Araújo WL, Sulpice R (2018) Nitrogen metabolism in cyanobacteria: metabolic and molecular control, growth consequences and biotechnological applications. Crit Rev Microbiol **44:** 541–560

Flores E, Herrero A (2004) Assimilatory nitrogen metabolism and its regulation. In DA Bryant, ed, The Molecular Biology of Cyanobacteria. Kluwer Academic Publishers, Dordrecht, Netherlands, pp 487–517

Forcada-Nadal A, Llácer JL, Contreras A, Marco-Marín C, Rubio V (2018) The PII-NAGK-PipX-NtcA regulatory axis of cyanobacteria: A tale of changing partners, allosteric effectors and non-covalent interactions. Front Mol Biosci **5:** 91

Forchhammer K, Schwarz R (2019) Nitrogen chlorosis in unicellular cyanobacteria—a developmental program for surviving nitrogen deprivation. Environ Microbiol **21:** 1173–1184

Forchhammer K, Selim KA (2020) Carbon/nitrogen homeostasis control in cyanobacteria. FEMS Microbiol Rev **44:** 33–53

Galmozzi CV, Fernández-Avila MJ, Reyes JC, Florencio FJ, Muro-Pastor MI (2007) The ammonium-inactivated cyanobacterial glutamine synthetase I is reactivated in vivo by a mechanism involving proteolytic removal of its inactivating factors. Mol Microbiol **65:** 166–179

García-Domínguez M, López-Maury L, Florencio FJ, Reyes JC (2000) A gene cluster involved in metal homeostasis in the cyanobacterium *Synechocystis* sp. strain PCC 6803. J Bacteriol **182:** 1507–1514

García-Domínguez M, Reyes JC, Florencio FJ (1999) Glutamine synthetase inactivation by protein–protein interaction. Proc Natl Acad Sci USA **96:** 7161–7166

García-Domínguez M, Reyes JC, Florencio FJ (1997) Purification and characterization of a new type of glutamine synthetase from cyanobacteria. Eur J Biochem **244:** 258–264

Giner-Lamia J, Robles-Rengel R, Hernández-Prieto MA, Muro-Pastor MI, Florencio FJ, Futschik ME (2017) Identification of the direct regulon of NtcA during early acclimation to nitrogen starvation in the cyanobacterium *Synechocystis* sp. PCC 6803. Nucleic Acids Res **45:** 11800–11820

Gründel M, Scheunemann R, Lockau W, Zilliges Y (2012) Impaired glycogen synthesis causes metabolic overflow reactions and affects stress responses in the cyanobacterium *Synechocystis* sp. PCC 6803. Microbiology (Reading) **158:** 3032–3043

Guerrero F, Carbonell V, Cossu M, Correddu D, Jones PR (2012) Ethylene synthesis and regulated expression of recombinant protein in *Synechocystis* sp. PCC 6803. PLoS One **7:** e50470

Gupta JK, Rai P, Jain KK, Srivastava S (2020) Overexpression of bicarbonate transporters in the marine cyanobacterium *Synechococcus* sp. PCC 7002 increases growth rate and glycogen accumulation. Biotechnol Biofuels **13:** 17

Hasunuma T, Kikuyama F, Matsuda M, Aikawa S, Izumi Y, Kondo A (2013) Dynamic metabolic profiling of cyanobacterial glycogen biosynthesis under conditions of nitrate depletion. J Exp Bot **64:** 2943–2954

Hauf W, Schmid K, Gerhardt EC, Huergo LF, Forchhammer K (2016) Interaction of the nitrogen regulatory protein GlnB (PII) with biotin carboxyl carrier protein (BCCP) controls acetyl-CoA levels in the cyanobacterium *Synechocystis* sp. PCC 6803. Front Microbiol **7:** 1700

Heinrikson RL, Meredith SC (1984) Amino acid analysis by reverse-phase high-performance liquid chromatography: precolumn derivatization with phenylisothiocyanate. Anal Biochem **136:** 65–74

Herrero A, Muro-Pastor AM, Flores E (2001) Nitrogen control in cyanobacteria. J Bacteriol **183:** 411–425

Kiyota H, Hirai MY, Ikeuchi M (2014) NblA1/A2-dependent homeostasis of amino acid pools during nitrogen starvation in *Synechocystis* sp. PCC 6803. Metabolites **4:** 517–531

Klotz A, Georg J, Bučinská L, Watanabe S, Reimann V, Januszewski W, Sobotka R, Jendrossek D, Hess WR, Forchhammer K (2016) Awakening of a dormant cyanobacterium from nitrogen chlorosis reveals a genetically determined program. Curr Biol **26:** 2862–2872

Knoop H, Zilliges Y, Lockau W, Steuer R (2010) The metabolic network of *Synechocystis* sp. PCC 6803: systemic properties of autotrophic growth. Plant Physiol **154:** 410–422

Kopf M, Klähn S, Scholz I, Matthiessen JKF, Hess WR, Voß B (2014) Comparative analysis of the primary transcriptome of *Synechocystis* sp. PCC 6803. DNA Res **21:** 527–539

Krasikov V, Aguirre von Wobeser E, Dekker HL, Huisman J, Matthijs HC (2012) Time-series resolution of gradual nitrogen starvation and its impact on photosynthesis in the cyanobacterium *Synechocystis* PCC 6803. Physiol Plant **145:** 426–439

Laemmli UK (1970) Cleavage of structural proteins during the assembly of the head of bacteriophage T4. Nature **227:** 680–685

López-Maury L, Florencio FJ, Reyes JC (2003) Arsenic sensing and resistance system in the cyanobacterium *Synechocystis* sp. strain PCC 6803. J Bacteriol **185:** 5363–5371

Lowry OH, Rosebrough NJ, Farr AL, Randall RJ (1951) Protein measurement with the Folin phenol reagent. J Biol Chem **193:** 265–275

Luan G, Zhang S, Wang M, Lu X (2019) Progress and perspective on cyanobacterial glycogen metabolism engineering. Biotechnol Adv **37:** 771–786

Mackinney G (1941) Absorption of light by chlorophyll solutions. J Biol Chem **140:** 315–322

Marqués S, Mérida A, Candau P, Florencio FJ (1992) Light-mediated regulation of glutamine synthetase activity in the unicellular cyanobacterium *Synechococcus* sp. PCC 6301. Planta **187:** 247–253

Mérida A, Candau P, Florencio FJ (1991) Regulation of glutamine synthetase activity in the unicellular cyanobacterium *Synechocystis* sp. strain PCC 6803 by the nitrogen source: Effect of ammonium. J Bacteriol **173:** 4095–4100

Mitschke J, Vioque A, Haas F, Hess WR, Muro-Pastor AM (2011) Dynamics of transcriptional start site selection during nitrogen stress-induced cell differentiation in *Anabaena* sp. PCC7120. Proc Natl Acad Sci USA **108:** 20130–20135

Möllers KB, Cannella D, Jørgensen H, Frigaard NU (2014) Cyanobacterial biomass as carbohydrate and nutrient feedstock for bioethanol production by yeast fermentation. Biotechnol Biofuels **7:** 64

Muro-Pastor MI, Reyes JC, Florencio FJ (2005) Ammonium assimilation in cyanobacteria. Photosynth Res **83:** 135–150

Muro-Pastor MI, Reyes JC, Florencio FJ (2001) Cyanobacteria perceive nitrogen status by sensing intracellular 2-oxoglutarate levels. J Biol Chem **276:** 38320–38328

Oliver NJ, Rabinovitch-Deere CA, Carroll AL, Nozzi NE, Case AE, Atsumi S (2016) Cyanobacterial metabolic engineering for biofuel and chemical production. Curr Opin Chem Biol **35:** 43–50

Osanai T, Imamura S, Asayama M, Shirai M, Suzuki I, Murata N, Tanaka K (2006) Nitrogen induction of sugar catabolic gene expression in *Synechocystis* sp. PCC 6803. DNA Res **13:** 185–195

Osanai T, Oikawa A, Iijima H, Kuwahara A, Asayama M, Tanaka K, Ikeuchi M, Saito K, Hirai MY (2014a) Metabolomic analysis reveals rewiring of *Synechocystis* sp. PCC 6803 primary metabolism by ntcA overexpression. Environ Microbiol **16:** 3304–3317

Osanai T, Oikawa A, Shirai T, Kuwahara A, Iijima H, Tanaka K, Ikeuchi M, Kondo A, Saito K, Hirai MY (2014b) Capillary electrophoresis-mass spectrometry reveals the distribution of carbon metabolites during nitrogen starvation in *Synechocystis* sp. PCC 6803. Environ Microbiol **16:** 512–524

Pettersen EF, Goddard TD, Huang CC, Couch GS, Greenblatt DM, Meng EC, Ferrin TE (2004) UCSF Chimera—a visualization system for exploratory research and analysis. J Comput Chem **25:** 1605–1612

Prentki P, Krisch HM (1984) In vitro insertional mutagenesis with a selectable DNA fragment. Gene **29:** 303–313

Qian X, Zhang Y, Lun DS, Dismukes GC (2018) Rerouting of metabolism into desired cellular products by nutrient stress: Fluxes reveal the selected pathways in cyanobacterial photosynthesis. ACS Synth Biol **7:** 1465–1476

Reyes JC, Crespo JL, García-Domínguez M, Florencio FJ (1995) Electron transport controls glutamine synthetase activity in the facultative heterotrophic cyanobacterium *Synechocystis* sp. PCC 6803. Plant Physiol **109:** 899–905

Rippka R (1988) Isolation and purification of cyanobacteria. Methods Enzymol **167:** 3–27

Sato S, Shimoda Y, Muraki A, Kohara M, Nakamura Y, Tabata S (2007) A large-scale protein interaction analysis in *Synechocystis* sp. PCC6803. DNA Res **14:** 207–216

Scholl J, Dengler L, Bader L, Forchhammer K (2020) Phosphoenolpyruvate carboxylase from the cyanobacterium Synechocystis sp. PCC 6803 is under global metabolic control by P_{II} signaling. Mol Microbiol **114:** 292–307

Schwarz D, Orf I, Kopka J, Hagemann M (2014) Effects of inorganic carbon limitation on the metabolome of the *Synechocystis* sp. PCC 6803 mutant defective in glnB encoding the central regulator PII of cyanobacterial C/N acclimation. Metabolites **4:** 232–247

Shimakawa G, Hasunuma T, Kondo A, Matsuda M, Makino A, Miyake C (2014) Respiration accumulates Calvin cycle intermediates for the rapid start of photosynthesis in *Synechocystis* sp. PCC 6803. Biosci Biotechnol Biochem **78:** 1997–2007

Song Y, DiMaio F, Wang RYR, Kim D, Miles C, Brunette T, Thompson J, Baker D (2013) High-resolution comparative modeling with RosettaCM. Structure **21:** 1735–1742

Spät P, Klotz A, Rexroth S, Maček B, Forchhammer K (2018) Chlorosis as a developmental program in cyanobacteria: The proteomic fundament for survival and awakening. Mol Cell Proteomics **17:** 1650–1669

Spät P, Maček B, Forchhammer K (2015) Phosphoproteome of the cyanobacterium *Synechocystis* sp. PCC 6803 and its dynamics during nitrogen starvation. Front Microbiol **6:** 248

Watzer B, Spät P, Neumann N, Koch M, Sobotka R, Macek B, Hennrich O, Forchhammer K (2019) The signal transduction protein PII controls ammonium, nitrate and urea uptake in cyanobacteria. Front Microbiol **10:** 1428

Xiong W, Cano M, Wang B, Douchi D, Yu J (2017) The plasticity of cyanobacterial carbon metabolism. Curr Opin Chem Biol **41:** 12–19

Xu Y, Guerra LT, Li Z, Ludwig M, Dismukes GC, Bryant DA (2013) Altered carbohydrate metabolism in glycogen synthase mutants of *Synechococcus* sp. strain PCC 7002: Cell factories for soluble sugars. Metab Eng **16:** 56–67

Yamauchi Y, Kaniya Y, Kaneko Y, Hihara Y (2011) Physiological roles of the cyAbrB transcriptional regulator pair Sll0822 and Sll0359 in *Synechocystis* sp. strain PCC 6803. J Bacteriol **193:** 3702–3709

Zavřel T, Očenášová P, Červený J (2017) Phenotypic characterization of *Synechocystis* sp. PCC 6803 substrains reveals differences in sensitivity to abiotic stress. PLoS One **12:** e0189130

Zhang CC, Zhou CZ, Burnap RL, Peng L (2018) Carbon/nitrogen metabolic balance: Lessons from cyanobacteria. Trends Plant Sci **23:** 1116–1130